

GroEL/ES inhibitors as potential antibiotics

Sanofar Abdeen,^a Nilshad Salim,^a Najiba Mammadova,^{a,f} Corey Summers,^{a,g} Rochelle Frankson,^{a,h} Andrew J. Ambrose,^b Gregory G. Anderson,^c Peter G. Schultz,^d Arthur L. Horwich,^e Eli Chapman,^b and Steven M. Johnson^{a*}

^a Indiana University, School of Medicine, Department of Biochemistry and Molecular Biology, 635 Barnhill Dr., Indianapolis, IN 46202

^b The University of Arizona, College of Pharmacy, Department of Pharmacology and Toxicology, 1703 E. Mabel St., PO Box 210207, Tucson, AZ 85721

^c Indiana University-Purdue University Indianapolis, Department of Biology, 723 W. Michigan St., Indianapolis, IN 46202

^d The Scripps Research Institute, Department of Chemistry, 10550 North Torrey Pines Rd., La Jolla, CA 92037

^e HHMI, Department of Genetics, Yale School of Medicine, Boyer Center for Molecular Medicine, 295 Congress Ave., New Haven, CT 06510

Present addresses:

^f Department of Genetics, Development and Cell Biology, Iowa State University, 1210 Molecular Biology Building, Pannel Dr, Ames, IA 50011

^g Department of Kinesiology, Iowa State University, 235 Barbara E. Forker Building, Beach Rd, Ames, IA 50011

^h Department of Medicinal Chemistry and Molecular Pharmacology, Purdue University, Hansen Life Sciences Research Building, 201 S. University Street, West Lafayette, IN 47907

*Correspondence: johnstm@iu.edu, Tel: 317-274-2458, Fax: 317-274-4686

KEYWORDS. GroEL, GroES, HSP60, HSP10, molecular chaperone, chaperonin, proteostasis, small molecule inhibitors, *ESKAPE* pathogens, antibiotics.

This is the author's manuscript of the article published in final edited form as:

Abdeen, S., Salim, N., Mammadova, N., Summers, C. M., Frankson, R., Ambrose, A. J., ... Johnson, S. M. (2016). GroEL/ES inhibitors as potential antibiotics. *Bioorganic & Medicinal Chemistry Letters*, 26(13), 3127–3134. <https://doi.org/10.1016/j.bmcl.2016.04.089>

Abstract:

We recently reported results from a high-throughput screening effort that identified 235 inhibitors of the *Escherichia coli* GroEL/ES chaperonin system [Johnson *et al.*, 2014]. As the GroEL/ES chaperonin system is essential for growth under all conditions, we reasoned that targeting GroEL/ES with small molecule inhibitors could be a viable antibacterial strategy. Extending from our initial screen, we report here the antibacterial activities of 22 GroEL/ES inhibitors against a panel of Gram-positive and Gram-negative bacteria, including *E. coli*, *Bacillus subtilis*, *Enterococcus faecium*, *Staphylococcus aureus*, *Klebsiella pneumoniae*, *Acinetobacter baumannii*, *Pseudomonas aeruginosa*, and *Enterobacter cloacae*. GroEL/ES inhibitors were more effective at blocking the proliferation of Gram-positive bacteria, in particular *S. aureus*, where lead compounds exhibited antibiotic effects from the low- μ M to mid-nM range. While several compounds inhibited the human HSP60/10 refolding cycle, some were able to selectively target the bacterial GroEL/ES system. Despite inhibiting HSP60/10, many compounds exhibited low to no cytotoxicity against human liver and kidney cell lines. Two lead candidates emerged from the panel, compounds **8** and **18**, that exhibit >50-fold selectivity for inhibiting *S. aureus* growth compared to liver or kidney cell cytotoxicity. Compounds **8** and **18** inhibited drug-sensitive and methicillin-resistant *S. aureus* strains with potencies comparable to vancomycin, daptomycin, and streptomycin, and are promising candidates to explore for validating the GroEL/ES chaperonin system as a viable antibiotic target.

The number of lives saved by antibiotics is a hallmark of the success of this class of drugs. However, resistant bacterial strains have been identified for every class of antibiotic, usually within a few years of general therapeutic use.¹⁻³ The threat of antibiotic resistance is epitomized by the emergence of six multi-drug resistant bacteria referred to as the *ESKAPE* pathogens: *Enterococcus faecium*, *Staphylococcus aureus*, *Klebsiella pneumoniae*, *Acinetobacter baumannii*, *Pseudomonas aeruginosa*, and *Enterobacter* species.⁴⁻⁸ The Center for Disease Control (CDC) Antibiotic Resistance Threat Report lists these bacteria as serious threats (level 4 out of 5) requiring prompt and sustained action.⁹ Most alarming is that antibiotic resistance has mounted to the point where therapeutics are severely limited or ineffective for once easily treated infections. For example, ~10,000 people per year are estimated to die from methicillin-resistant *S. aureus* (MRSA) infections in the United States.¹⁰ Moreover, the CDC estimates the direct medical cost of treating antibiotic resistant bacterial infections in the US is more than \$20 billion per year.⁹ Clearly, the rise of resistant bacterial strains requires enhanced research efforts to ensure an ongoing antibiotic pipeline.

Current antibiotics primarily function by blocking cell wall construction, structure and function of the cell membrane, protein synthesis, DNA structure and function, or folic acid synthesis.¹¹ Recently developed therapeutics for infections caused by drug-resistant bacteria include the injectable carbapenem beta-lactam, doripenem, which targets penicillin-binding proteins and inhibits cell wall synthesis;¹² the cyclic lipopeptide, daptomycin, which inserts into the bacterial membrane and leads to pore formation;¹³ quinupristin/dalfopristin, which bind to two different sites on the 50S ribosomal subunit and interfere with protein synthesis;¹⁴ the oxazolidinone, linezolid, which also binds the 50S ribosomal subunit;¹⁵ the tetracycline derivative, tigecycline, which targets protein synthesis via the 30S ribosomal subunit;¹⁶ and the

lipoglycopeptide, dalbavancin, which has the same mode of action as vancomycin, binding to the D-Ala-D-Ala motif in the cell wall.¹⁷ As these examples illustrate, most new antibiotics are derivatives of existing drugs that also target the aforementioned pathways. Unfortunately, bacterial resistance to these drugs is quick to develop. These data argue for the continued pursuit of antibiotics with entirely new modes of action, which may better avoid mechanisms of resistance and have longer effective life times.

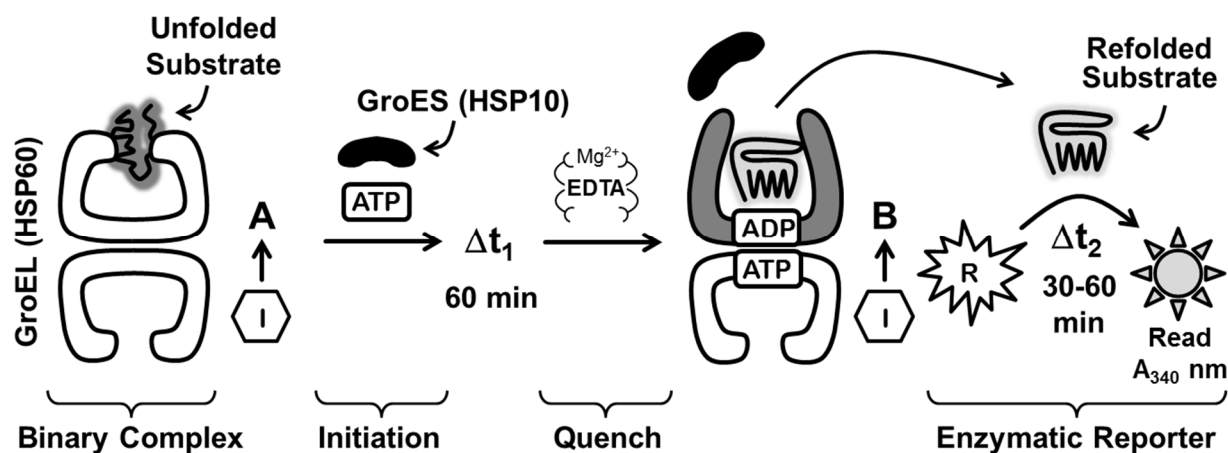


Figure 1. General protocol for chaperonin-mediated biochemical assays. Compounds (I) are added at point A to a solution containing GroEL (or HSP60) with bound substrate protein (e.g. malate dehydrogenase, MDH). Addition of GroES (or HSP10) and ATP initiates the refolding cycle, which is quenched with EDTA after a 60 minute incubation. Substrates (R) for the refolded reporter enzyme are added and after another 30-60 minute incubation (until the DMSO control wells have reached ~90% consumption of NADH), absorbance is measured to evaluate the amount of refolded enzyme present, and by association the extent of chaperonin inhibition. Alternatively, addition of compounds at point B enables determination of off-target inhibition of the reporter enzyme (i.e. native MDH enzyme activity). Chaperonin-mediated ATP hydrolysis is also evaluated using a malachite green assay. Biochemical assays employing Rhodanese (Rho) are performed similarly (refer to the Supporting Information for detailed protocols).

An attractive strategy for the development of novel antibiotics is to target bacterial protein homeostasis (proteostasis) mechanisms, in particular molecular chaperones. Molecular chaperones are a specialized class of proteins that help other proteins to properly fold to their native states. Among the molecular chaperones in *E. coli*, the GroEL/ES chaperonin system is the only one essential for growth under all conditions.^{18, 19} GroEL is a central processing

machine that maintains the structural and functional integrity of many other proteins (**Figure 1**); for a review, see references 19 and 20.¹⁹⁻²² Thus, targeting this one functional node results in a cascading effect that leads to the dysfunction of numerous key cellular pathways, which is lethal to bacteria.¹⁸ Because no other drugs function by targeting chaperonin systems, this strategy should be effective against bacteria that are resistant to current antibiotics.

The central tenet of this antibiotic strategy raises the question of whether bacterial GroEL/ES can be targeted specifically without interfering with the metazoan counterpart in the mitochondria, HSP60/10, whose partial deficiency in humans leads to disease.²³ Human HSP60 shares 48% sequence identity with *E. coli* GroEL, and thus there is the possibility of inhibitor cross-talk between the two chaperonins. However, structural and functional differences between the two systems suggest that it should be possible to develop inhibitors that selectively target bacterial GroEL/ES over human HSP60/10. GroEL is a homo-tetradecameric protein consisting of two, seven-membered rings that stack back-to-back.²⁴⁻²⁶ Through a series of events driven by ATP binding and hydrolysis, unfolded substrate proteins are bound within the central cavity of one GroEL ring and encapsulated by the heptameric GroES co-chaperonin lid structure, triggering protein folding in a sequestered chamber.²⁵⁻³¹ GroEL/ES works as an allosterically-controlled, double-ring system, which is regulated through positive intra-ring ATP-binding and negative inter-ring binding. In contrast, studies have indicated that human HSP60/10 operates as a single-ring species, through at least part of the cycle, removing many of the intermediate states associated with the GroEL/ES refolding cycle.³²⁻³⁴ Thus, it should be possible to develop inhibitors that selectively target the double-ring GroEL/ES cycle with its additional allosteric signals and conformational intermediates. Furthermore, HSP60/10 is in the mitochondrial matrix, which is often protected from small molecule penetration; thus, even if compounds are

found that inhibit HSP60/10 in biochemical assays, they may not display cytotoxicity if they failed to reach the mitochondrial matrix.

We previously developed a series of compounds that bind to the ATP sites of *E. coli* GroEL and inhibit the chaperonin refolding cycle.^{35,36} We also conducted a high-throughput screen to discover inhibitors of the *E. coli* GroEL/ES chaperonin system that target sites other than the ATP pockets, as we had concerns that ATP-competitive inhibitors may have off-target effects against other ATP-dependent proteins in cells.³⁷ We chose the *E. coli* GroEL/ES homolog for screening because it is the best characterized chaperonin and has been a model system for studying this class of proteins.^{30,31,38-40} It shares high homology with GroEL/ES systems from other bacteria, with 56-97% identical amino acids for GroEL and 44-94% identical amino acids for GroES (refer to **Table S1** in the Supporting Information). Thus, *E. coli* GroEL/ES serves as an excellent surrogate to discover chaperonin inhibitors to treat bacterial infections. The assays we developed analyzed the full refolding cycle and used the substrate reporter enzymes β -arylsulfotransferase IV (AST-IV) and malate dehydrogenase (MDH), which require GroEL, GroES, and ATP in order to return to their native, active states (refer to **Figure 1** for a general overview of the assay protocols). From ~700,000 molecules, our high-throughput screening narrowed the number of GroEL/ES inhibitors to 235. We investigated a subset of these hits in greater detail to identify IC₅₀ values for inhibiting GroEL/ES-mediated substrate refolding and ATPase activity. While only a few compounds inhibited GroEL/ES-mediated ATPase activity, most were potent inhibitors of the refolding cycle and exhibited minimal to no off-target effects against the reporter enzyme.³⁷

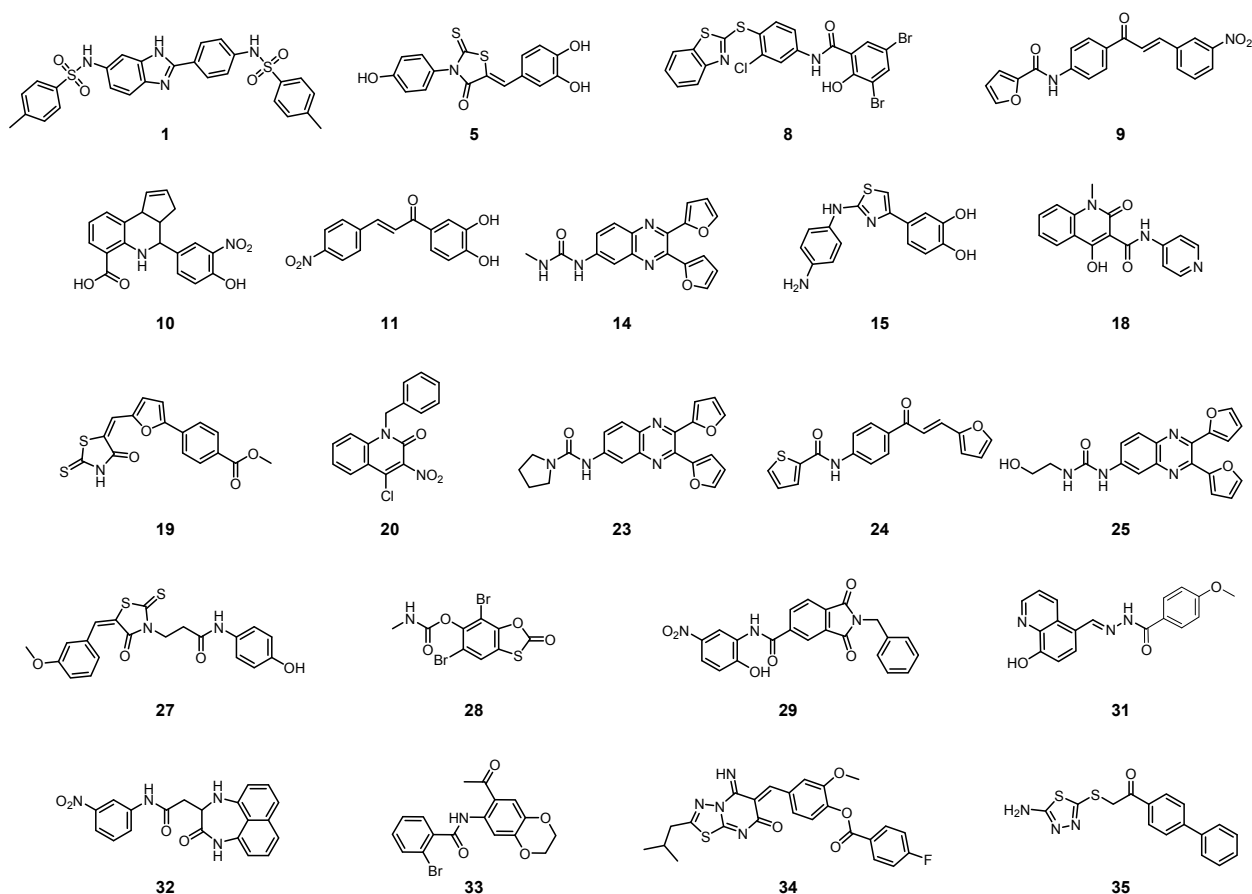


Figure 2. Structures of the 22 compounds under evaluation. For ease of comparison, compound numbering from **1-36** was maintained as presented in our previous high-throughput screening study.³⁷ Compounds **2-4**, **6**, **7**, **12**, **13**, **16**, **17**, **21**, **22**, **26**, **30**, and **36** were omitted from evaluation as they were either not commercially available, or purchased compounds were not readily identified by LC-MS and/or did not have acceptable purities confirmed by HPLC.

Extending from our high-throughput screening studies, we have been investigating the antibiotic potential of 22 of our initial GroEL/ES inhibitor hits (**Figure 2**). We first tested the GroEL/ES inhibitors in two additional biochemical counter-screens to further support that they are acting “on-target” and are not simply artifacts or false-positives. The first counter-screen evaluates for inhibition of GroEL/ES-mediated refolding of a third stringent substrate, Rhodanese (Rho). The second counter-screen evaluates for inhibition of the native Rho enzymatic reporter reaction. Detailed protocols for these two assays are presented in the Supporting Information).⁴¹⁻⁴⁴ For most of the compounds, we found a direct correlation between

inhibition of both the GroEL/ES-mediated dMDH and dRho refolding reactions (**Table 1** and **Figure 3A**). While some compounds inhibited either the native MDH or Rho reporter reactions, only compound **10** inhibited in both counter-screens, and only to a minor extent against native MDH (**Table 1** and **Figure 3B**). Thus, we are confident that compounds are on-target inhibitors of dMDH and dRho refolding. We next evaluated the 22 compounds for their antibiotic effects on *E. coli* cells. A general bacterial proliferation assay (see the Supporting Information for a detailed protocol) was employed in liquid media using DH5 α *E. coli* cells as the initial test strain (EC₅₀ values are summarized in **Table 2** and graphically in **Figure 4A**). Unfortunately, no significant inhibition of bacterial growth was observed for any of the compounds up to 100 μ M. Reasoning this might be due to efflux of the molecules, we tested against an MC4100 Δ *acrB* *E. coli* strain, which has one of the central components of the AcrA/AcrB/TolC efflux pump removed.^{45, 46} Compounds **8** and **18** were the most potent inhibitors of this efflux-compromised *E. coli* strain (EC₅₀ = 2.3 and 21 μ M, respectively), with the remainder of the compounds being inactive.

Table 1. Biochemical IC₅₀ results for *E. coli* GroEL/ES inhibitors. Statistical analyses (two-tailed t-tests) were performed for compound log(IC₅₀) values determined from the GroEL/ES-dRho and GroEL/ES-dMDH refolding assays. Compounds for which there is a statistically significant difference between inhibition results have been marked with a “★” between the two assay results being compared ($p < 0.05$). P-values could not be calculated for compounds marked with a “#” as one IC₅₀ is greater than the maximum compound concentration tested. For most compounds, IC₅₀ values are not statistically different (17/22 compounds), suggesting they are “on-target” for inhibiting the refolding of the dRho and dMDH substrates. IC₅₀ correlations are represented graphically in **Figure 3**.

Biochemical Assay IC ₅₀ Values (μM)						
#	Native Rho Reporter Activity	Native MDH Reporter Activity	GroEL/ES-dRho Refolding		GroEL/ES-dMDH Refolding	GroEL/ES-dMDH ATPase
1	>100	>62.5	30	*	7.5	119
5	14	>62.5	0.58		0.69	>250
8	>100	7.1	1.4		1.4	>250
9	>100	>62.5	1.4		0.93	80
10	0.25	54	0.47		0.80	174
11	12	>62.5	0.83		1.2	216
14	2.5	>62.5	2.5		3.0	>250
15	23	>62.5	1.7		2.7	>250
18	>100	>62.5	6.8		5.7	>250
19	8.1	>62.5	3.0		4.8	>250
20	>100	>62.5	22	*	5.4	>250
23	2.1	>62.5	2.4		4.7	>250
24	>100	>62.5	2.3		3.6	>250
25	1.4	>62.5	2.6		6.5	>250
27	12	>62.5	9.6	*	4.7	>250
28	5.3	>62.5	0.89		2.6	>250
29	>100	>62.5	28		24	187
31	52	>62.5	18		31	>250
32	10	>62.5	11	*	42	217
33	>100	>62.5	>250		>100	>250
34	>100	>62.5	25		24	>250
35	>100	>62.5	79	#	>100	107

IC₅₀ = Inhibitor Concentration resulting in 50% reduction of biochemical activity

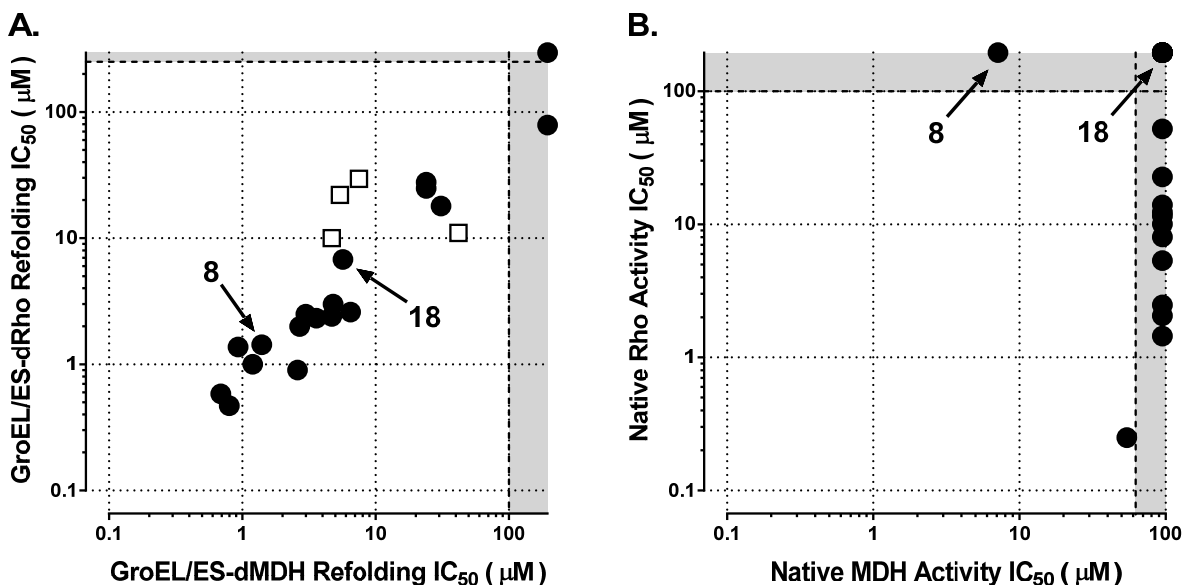


Figure 3. **A.** Compounds inhibit nearly equipotently in the *E. coli* GroEL/ES-dMDH and the GroEL/ES-dRho refolding assays. Data plotted in the grey zones represent results beyond the assay detection limits (i.e. >100 μM for the dMDH refolding assay, and >250 μM for the dRho refolding assay). Compounds indicated by the white squares are those with statistically significant differences between their IC₅₀ values ($p < 0.05$). **B.** While some compounds inhibit either native MDH or Rho individually, only compound **10** inhibits in both counter-screens, and only to a minor extent against native MDH. Data plotted in the grey zones represent results

beyond the assay detection limits (i.e. >62.5 μM for the native MDH enzymatic reporter assay, and >100 μM for the native Rho enzymatic reporter assay).

That many of the most potent GroEL/ES biochemical inhibitors were ineffective against the MC4100 ΔacrB *E. coli* cells could be due to the presence of other efflux pumps that were still functional, as it is known that *E. coli* contains several classes of efflux pumps.⁴⁷⁻⁵⁰ However, another possibility is that the molecules were not able to traverse the highly impermeable lipopolysaccharide (LPS) outer membrane characteristic of Gram-negative bacteria. To probe this, we tested the compounds against a mutant SM101 *lpxA2* *E. coli* strain, which has a temperature sensitive LpxA allele leading to compromised LPS biosynthesis at non-permissive temperatures, and consequently a greater permeability to molecules.^{51, 52} We found that 10 compounds inhibited the growth of this *E. coli* strain, with compounds **8** and **18** still proving to be the most effective (EC₅₀ values of 0.33 and 3.3 μM , respectively). These results were further supported by the ability of many compounds to inhibit the growth of a Gram-positive bacterium, *Bacillus subtilis* (**Table 2** and **Figure 4B**), which does not contain an LPS outer membrane. That more compounds failed to inhibit either the SM101 *lpxA2* *E. coli* or *B. subtilis* bacteria is putatively because of the presence of efflux pumps that were still intact for these strains, and/or the continued impermeability of compounds across the cell membranes.

Table 2. *E. coli* and *B. subtilis* bacterial proliferation EC₅₀ results for GroEL/ES inhibitors.

#	Bacterial Proliferation EC ₅₀ Values (μM)			
	DH5α <i>E. coli</i>	MC4100 Δ <i>AcrB</i> <i>E. coli</i>	SM101 <i>E. coli</i>	<i>B. subtilis</i>
1	>100	>100	>100	>100
5	>100	92	27	25
8	>100	2.3	0.33	0.10
9	>100	>100	76	>100
10	>100	>100	>100	>100
11	>100	>100	48	>100
14	>100	>100	>100	>100
15	>100	>100	84	>100
18	>100	21	3.3	0.47
19	>100	>100	7.6	16
20	>100	>100	>100	2.8
23	>100	>100	>100	>100
24	>100	>100	>100	>100
25	>100	>100	>100	>100
27	>100	>100	>100	>100
28	>100	>100	>100	43
29	>100	>100	>100	>100
31	>100	>100	19	83
32	>100	>100	68	72
33	>100	>100	>100	>100
34	>100	>100	25	13
35	>100	>100	>100	>100

EC₅₀ = Effective Concentration of compound resulting in 50% reduction of bacterial proliferation

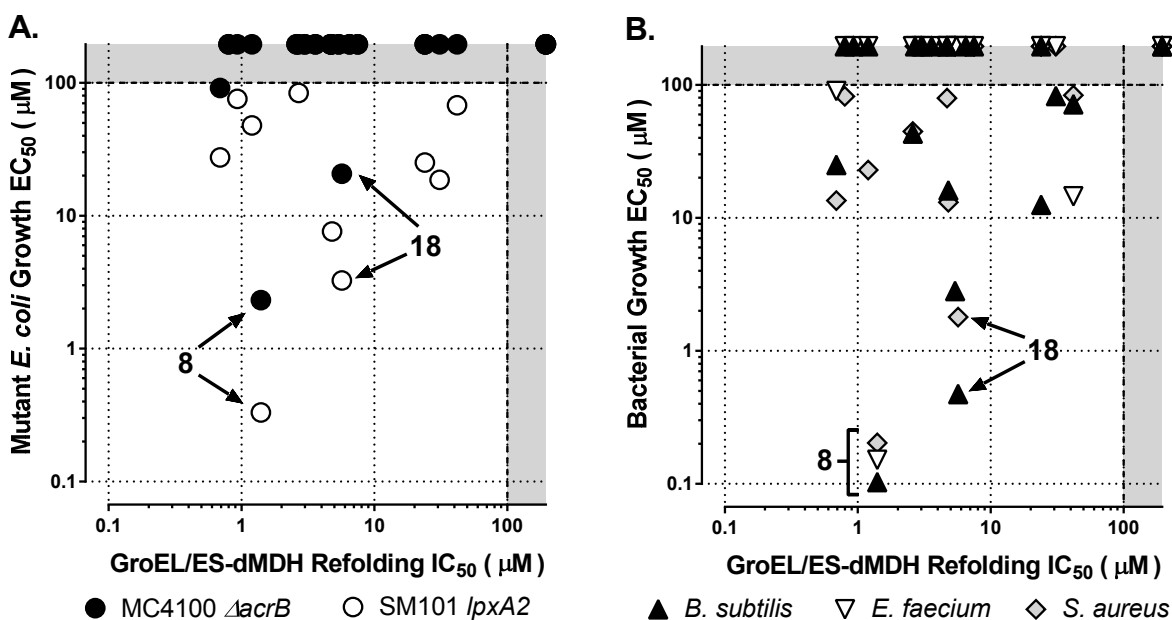


Figure 4. **A.** Inhibitors of the *E. coli* GroEL/ES-dMDH refolding cycle are inactive against parent *E. coli* bacteria; however, several exhibit antibacterial effects against mutant *E. coli* strains with compromised efflux pumps (MC4100 Δ*acrB*) and lipopolysaccharide (LPS) outer membranes (SM101 *lpxA2*). **B.** Parent *B. subtilis*, *E. faecium*, and *S. aureus* Gram-positive bacteria are more susceptible to the antibiotic effects of GroEL/ES inhibitors. Compound **8**

potently inhibits the growth of all three strains, while compound **18** is potent against *B. subtilis* and *S. aureus*, but inactive against *E. faecium*. Data plotted in the grey zones represent results beyond the assay detection limits (i.e. >100 μM).

While *E. coli* and *B. subtilis* were good model systems for initial proof-of-principle studies, we wanted to elucidate the antibiotic potential of our GroEL/ES inhibitors against a panel of more clinically relevant bacteria, in particular the *ESKAPE* pathogens. We adapted the general bacterial proliferation assay to test molecules against *E. faecium*, *S. aureus* (plus an MRSA strain), *K. pneumoniae*, *A. baumannii*, *P. aeruginosa*, and *E. cloacae* (see the Supporting Information for detailed protocols). A summary of the EC_{50} values for compounds against these bacteria is presented in **Table 3** (and graphically in **Figure 4B**), with a comparison against several common antibiotics. As four of the *ESKAPE* pathogens are Gram-negative (*K. pneumoniae*, *A. baumannii*, *P. aeruginosa*, and *E. cloacae*), it is not surprising that the GroEL/ES inhibitors were largely ineffective against them. The remaining two *ESKAPE* pathogens, *E. faecium* and *S. aureus*, are Gram-positive bacteria. Compound **8** was very potent at inhibiting *E. faecium* growth (EC_{50} = 0.15 μM), and compound **32** was moderately potent (EC_{50} = 15 μM). Somewhat surprisingly, compound **18**, which emerged as a lead inhibitor against the *E. coli* and *B. subtilis* cells, was inactive against *E. faecium*. The remaining compounds were ineffective against *E. faecium*, which again supports the notion that the presence of an LPS membrane is not the sole determinant leading to compound inactivity. While compounds **8** and **18** emerged as the lead inhibitors of *S. aureus* growth (EC_{50} = 0.20 μM and 1.8 μM , respectively), four other compounds were also moderately effective with EC_{50} values between 10-50 μM (**5**, **11**, **19**, and **28**). To determine if they were bactericidal or bacteriostatic, we analyzed lead compounds **8** and **18** against the methicillin susceptible *S. aureus* strain (ATCC 25923) and found that both were acting as bactericidal inhibitors (refer to **Figure S1** in the

Supporting Information). We further tested compounds against an MRSA strain (ATCC #BAA-44: HPV107 strain, SCCmec Type I, Iberian PFGE Type) and found a correlation with the methicillin susceptible *S. aureus* strain (**Table 3**).

Table 3. EC₅₀ results for GroEL/ES inhibitors against the *ESKAPE* pathogens.

#	Bacterial Proliferation EC ₅₀ Values (μM)						
	<i>E. faecium</i>	<i>S. aureus</i>	MRSA	<i>K. pneumoniae</i>	<i>A. baumannii</i>	<i>P. aeruginosa</i>	<i>E. cloacae</i>
1	>100	>100	>100	>100	>100	>100	>100
5	90	14	9.1	>100	58	>100	>100
8	0.15	0.20	0.13	>100	30	>100	>100
9	>100	>100	>100	>100	>100	>100	>100
10	>100	82	>100	>100	>100	>100	>100
11	>100	23	40	>100	>100	>100	>100
14	>100	>100	94	>100	>100	>100	>100
15	>100	>100	>100	>100	81	>100	>100
18	>100	1.8	1.3	>100	>100	>100	>100
19	>100	13	1.5	>100	>100	>100	>100
20	>100	>100	21	>100	>100	>100	>100
23	>100	>100	>100	>100	>100	>100	>100
24	>100	>100	61	>100	>100	>100	>100
25	>100	>100	>100	>100	>100	>100	>100
27	>100	80	>100	>100	>100	>100	>100
28	>100	45	74	>100	>100	>100	>100
29	>100	>100	15	>100	>100	85	>100
31	>100	>100	56	95	32	>100	>100
32	15	84	54	>100	>100	>100	>100
33	>100	>100	>100	>100	>100	>100	>100
34	>100	>100	>100	>100	>100	>100	>100
35	>100	>100	>100	>100	>100	>100	>100
Ampicillin	0.63	0.059	76	89	2.5	27	>100
Minocycline	<0.05	<0.05	0.35	0.70	<0.05	2.4	1.5
Rifampicin	1.2	<0.05	0.15	5.4	0.47	5.2	6.2
Chloramphenicol	2.1	2.2	2.3	1.4	65	16	2.2
Kanamycin	>100	8.2	>100	45	16	25	37
Streptomycin	50	3.6	>100	3.4	>100	2.9	>100
Vancomycin	0.30	0.20	0.17	>100	17	74	>100
Daptomycin	33	5.7	5.7	>100	>100	>100	>100

EC₅₀ = Effective Concentration of compound resulting in 50% reduction of bacterial proliferation

While we have identified numerous inhibitors of GroEL/ES biochemical function, several of which we now know inhibit the growth of pathogenic bacteria (in particular *S. aureus* and MRSA), there remained the possibility that these compounds could be toxic to host cells owing to targeting of HSP60/10. To account for this possibility, *in vitro* counter-screens were carried out in analogous chaperonin-mediated dMDH refolding and ATPase biochemical assays employing HSP60/10 (**Table 4**). As indicated in **Figure 5A**, there was a correlation observed for

inhibiting both *E. coli* GroEL/ES and human HSP60/10; however, compounds were generally more potent at inhibiting *E. coli* GroEL/ES. Notably, compounds **1** and **18** displayed 12-fold and >17-fold selectivities, respectively, for inhibiting *E. coli* GroEL/ES over human HSP60/10. Unfortunately, the other lead inhibitor against *S. aureus* and MRSA bacteria, compound **8**, was only 4-fold selective. Thus, we were concerned about the cytotoxicity against human cells of **8** and other compounds that inhibited the HSP60/10 refolding cycle.

Table 4. Human HSP60/10 biochemical IC₅₀ and liver and kidney cytotoxicity EC₅₀ results for the GroEL/ES inhibitors. Statistical analyses (two-tailed t-tests) were performed for compound log(IC₅₀) values determined from the GroEL/ES-dMDH and HSP60/10-dMDH refolding assays. Compounds for which there is a statistically significant difference between inhibition results have been marked with a “★” between the two assay results being compared (p < 0.05). P-values could not be calculated for compounds marked with a “#” as one IC₅₀ is greater than the maximum compound concentration tested. IC₅₀ correlations are represented graphically in **Figure 5A**.

#	Biochemical Assay IC ₅₀ Values (μM)			Human Cell Viability EC ₅₀ Values (μM)		
	GroEL/ES-dMDH Refolding	HSP60/10-dMDH Refolding	HSP60/10-dMDH ATPase	THLE-3 (Liver)	HEK 293 (Kidney)	
1	7.5	★	89	106	29	34
5	0.69	★	4.9	>250	16	23
8	1.4	★	5.5	3.6	12	78
9	0.93		1.6	>250	>100	>100
10	0.80	★	3.3	140	>100	>100
11	1.2	★	5.2	>250	9.9	12
14	3.0		7.4	>250	>100	>100
15	2.7		10	>250	>100	98
18	5.7	#	>100	>250	>100	>100
19	4.8		16	>250	41	44
20	5.4		2.8	>250	3.6	17
23	4.7		13	>250	>100	>100
24	3.6		8.2	>250	34	55
25	6.5		15	>250	>100	>100
27	4.7	★	13	>250	>100	>100
28	2.6		1.8	>250	>100	>100
29	24	★	38	>250	>100	>100
31	31	#	>100	>250	15	7.7
32	42	#	>100	>250	61	62
33	>100		>100	>250	>100	>100
34	24		26	>250	>100	>100
35	>100		>100	>250	>100	>100

IC₅₀ = Inhibitor Concentration resulting in 50% reduction of biochemical activity
 EC₅₀ = Effective Concentration of compound resulting in 50% reduction in cell viability

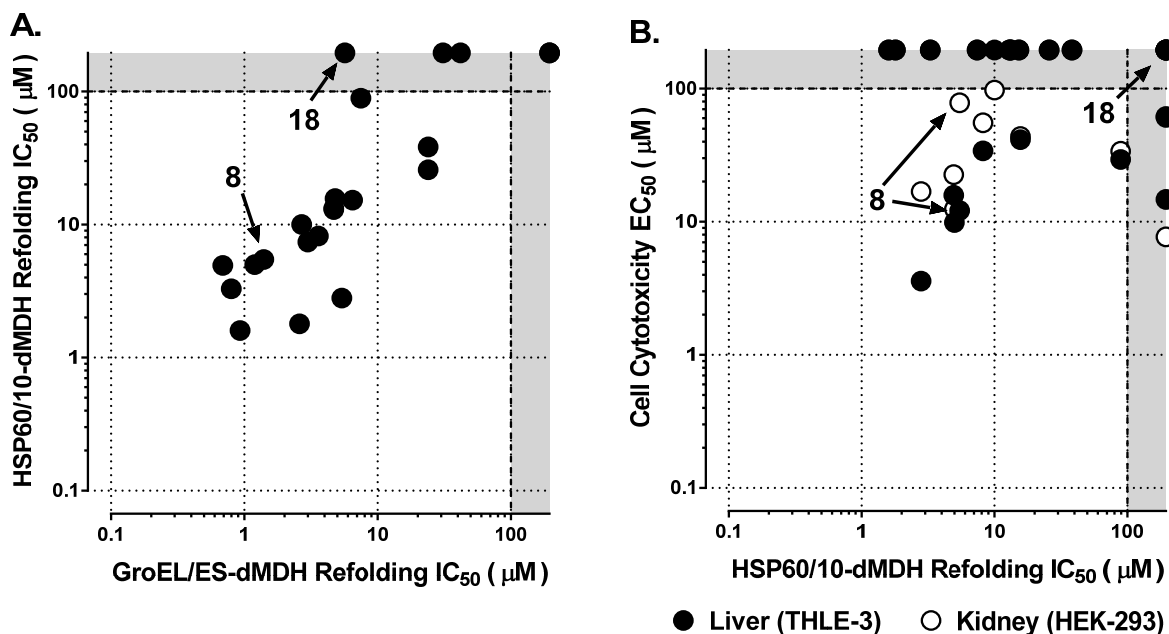


Figure 5. **A.** Compounds inhibit both *E. coli* GroEL/ES and human HSP60/10 chaperonin systems, but are generally more selective for the bacterial homolog. Compound **18** is inactive against human HSP60/10, whereas compound **8** exhibits low selectivity for GroEL/ES. **B.** Even though compounds can inhibit HSP60/10 biochemical function, many exhibit low or no cytotoxicity to human liver and kidney cells. Compound **18** exhibits no cytotoxicity, whereas compound **8** exhibits moderate or low toxicity. Data plotted in the grey zones represent results beyond the assay detection limits (i.e. >100 µM).

To gauge for potential cytotoxicity of chaperonin inhibitors to host tissues, we next evaluated compounds in viability assays using cultured human liver (THLE-3) and kidney (HEK 293) cells. These two stable cell lines were chosen because they are derived from the two main organs responsible for drug metabolism and excretion. An Alamar Blue-based cell viability assay was employed to probe for cytotoxicity.^{53, 54} We observed that inhibition of HSP60/10 biochemical activity did not directly translate into cell toxicity and that many compounds were only moderately toxic or non-toxic to both cell lines (**Table 4** and **Figure 5B**). This could be due to the fact that the inner mitochondrial membrane is highly impermeable to compounds, and thus inhibitors may not be able to penetrate to the mitochondrial matrix to reach HSP60/10. Compounds **8** and **18** were the most potent inhibitors of *S. aureus* proliferation, with the greatest

therapeutic windows compared to liver and kidney cell cytotoxicity (**Figure 6**). In particular, compound **8**, which exhibits an EC_{50} of 0.20 μM against *S. aureus* proliferation, has a therapeutic window of 60-fold with THLE-3 cells, and 390-fold with HEK 293 cells. Compound **18**, which exhibits an EC_{50} of 1.8 μM against *S. aureus* proliferation, is non-toxic to the liver and kidney cells up to the maximum concentrations tested ($EC_{50} > 100 \mu\text{M}$; therapeutic window > 55 -fold).

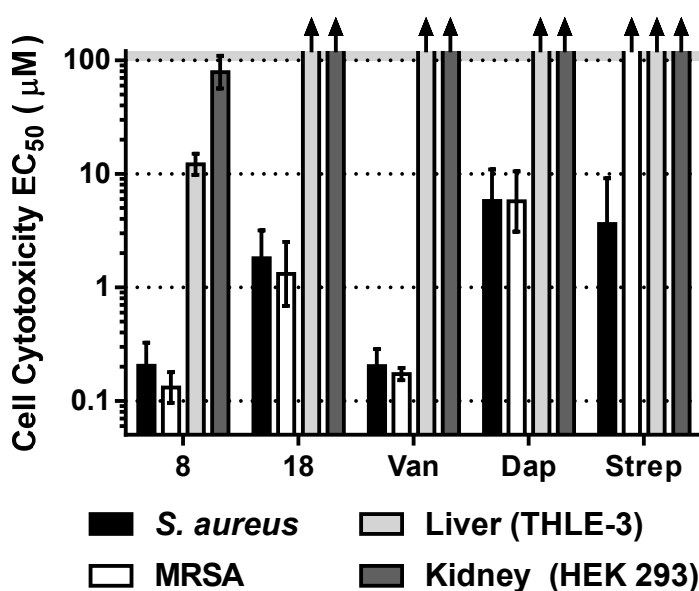


Figure 6. Compounds **8** and **18** are potent antibacterials against *S. aureus* & MRSA, with moderate/low to no toxicity to human liver and kidney cells. Results for Vancomycin (Van), Daptomycin (Dap), and Streptomycin (Strep) are shown for comparison. Arrows (↑) indicate EC_{50} results are $> 100 \mu\text{M}$ (the maximum concentrations tested).

In conclusion, we have investigated a subset of our previously identified inhibitors of the *E. coli* GroEL/ES chaperonin system for their antibiotic potential against a panel of bacteria including *E. coli* (3 strains), *B. subtilis*, *E. faecium*, *S. aureus* (including an MRSA strain), *K. pneumoniae*, *A. baumannii*, *P. aeruginosa*, and *E. cloacae*. The reported GroEL/ES inhibitors were largely ineffective at preventing the proliferation of the Gram-negative bacteria. While bacterial LPS outer membranes certainly play a significant role in preventing inhibitors from

penetrating these bacteria, our studies with the mutant MC4100 Δ *acrB* *E. coli* strain indicate that drug efflux is another contributing factor to inhibitor inactivation. Compounds **8** and **18** emerged as the lead candidate GroEL/ES inhibitors that exhibit >50-fold selectivity for blocking the growth of *S. aureus* bacteria versus human liver and kidney cytotoxicities. Their antibiotic efficacies against *S. aureus* are comparable to vancomycin, daptomycin, and streptomycin (**Figure 6**). Furthermore, they are effective against the MRSA strain evaluated here. We are pursuing further medicinal chemistry derivatization of these GroEL/ES inhibitors to develop lead analogs with more potent antibiotic effects against *S. aureus* (and ideally other bacteria) that remain non-toxic to mammalian cells. Since these inhibitors were discovered in a targeted GroEL/ES screen, we consider this the putative target, but we cannot rule out the possibility of off-target effects contributing to antibacterial potency. We are designing experiments to delineate the mechanism of action at the protein level and the mode of action at the whole cell level for these GroEL/ES inhibitors. The results presented here are encouraging, leading us to believe we can selectively target bacterial GroEL/ES chaperonin systems as an antibiotic strategy.

Supporting Information:

Supporting information associated with this article can be found in the online version, which includes tabulations of log(IC₅₀) and log(EC₅₀) results with standard deviations; experimental protocols for biochemical and cell-based assays; synthetic protocols and characterization data for compounds **10**, **15**, **23**, **24**, and **25**; and HPLC purity and MS characterization of test compounds.

Acknowledgments: We are grateful to the Genomics Institute of the Novartis Research Foundation for working with us on the previous high-throughput screening that initially identified these GroEL/ES biochemical inhibitors. We also thank Dr. Leendert Hamoen from the University of Amsterdam, Swammerdam Institute for Life Sciences (SILS) for the *B. subtilis* 168 cells. The human HSP60 expression plasmid (lacking the 26 amino acid *N*-terminal mitochondrial signal peptide) was generously donated by Dr. Abdussalam Azem from Tel Aviv University, Faculty of Life Sciences, Department of Biochemistry, Israel. We thank Dr. Quyen Hoang from the IU School of Medicine, Department of Biochemistry and Molecular Biology for helpful discussions and the use of various lab equipment. This work was supported in part by an IU Biomedical Research Grant, an IU Collaborative Research Grant, the Showalter Trust Foundation, and startup funds from the IU School of Medicine (SMJ) and the University of Arizona (EC).

References:

1. Clatworthy, A. E.; Pierson, E.; Hung, D. T. *Nature chemical biology* **2007**, *3*, 541.
2. Laxminarayan, R.; Duse, A.; Wattal, C.; Zaidi, A. K.; Wertheim, H. F.; Sumpradit, N.; Vlieghe, E.; Hara, G. L.; Gould, I. M.; Goossens, H.; Greko, C.; So, A. D.; Bigdeli, M.; Tomson, G.; Woodhouse, W.; Ombaka, E.; Peralta, A. Q.; Qamar, F. N.; Mir, F.; Kariuki, S.; Bhutta, Z. A.; Coates, A.; Bergstrom, R.; Wright, G. D.; Brown, E. D.; Cars, O. *Lancet Infect Dis* **2013**, *13*, 1057.
3. Davies, J.; Davies, D. *Microbiol Mol Biol Rev* **2010**, *74*, 417.
4. Rice, L. B. *J Infect Dis* **2008**, *197*, 1079.
5. Pendleton, J. N.; Gorman, S. P.; Gilmore, B. F. *Expert Rev Anti-Infe* **2013**, *11*, 297.
6. Boucher, H. W.; Talbot, G. H.; Bradley, J. S.; Edwards, J. E.; Gilbert, D.; Rice, L. B.; Scheld, M.; Spellberg, B.; Bartlett, J. *Clin Infect Dis* **2009**, *48*, 1.
7. Boucher, H. W.; Talbot, G. H.; Benjamin, D. K.; Bradley, J.; Guidos, R. J.; Jones, R. N.; Murray, B. E.; Bonomo, R. A.; Gilbert, D.; Amer, I. D. S. *Clin Infect Dis* **2013**, *56*, 1685.
8. Bassetti, M.; Merelli, M.; Temperoni, C.; Astilean, A. *Ann Clin Microb Anti* **2013**, *12*.
9. CDC. In *Antibiotic Resistance Threats in the United States, 2013*.; Centers for Disease Control and Prevention, 2013.
10. CDC. In *Active Bacterial Core Surveillance Report, Emerging Infections Program Network, Methicillin-Resistant Staphylococcus aureus, 2013*.; Centers for Disease Control and Prevention, 2013.
11. Walsh, C. *Antibiotics: Actions, Origins, Resistance*; Washington, DC: ASM Press, 2003.
12. Paterson, D. L.; Depestel, D. D. *Clin Infect Dis* **2009**, *49*, 291.
13. Steenbergen, J. N.; Alder, J.; Thorne, G. M.; Tally, F. P. *J Antimicrob Chemother* **2005**, *55*, 283.
14. Allington, D. R.; Rivey, M. P. *Clin Ther* **2001**, *23*, 24.
15. Shinabarger, D. L.; Marotti, K. R.; Murray, R. W.; Lin, A. H.; Melchior, E. P.; Swaney, S. M.; Dunyak, D. S.; Demyan, W. F.; Buysse, J. M. *Antimicrob Agents Chemother* **1997**, *41*, 2132.
16. Pankey, G. A. *J Antimicrob Chemother* **2005**, *56*, 470.
17. Scheinfeld, N. *Drugs Today (Barc)* **2007**, *43*, 305.
18. Fayet, O.; Ziegelhoffer, T.; Georgopoulos, C. *Journal of bacteriology* **1989**, *171*, 1379.
19. Chapman, E.; Farr, G. W.; Usaite, R.; Furtak, K.; Fenton, W. A.; Chaudhuri, T. K.; Hondorp, E. R.; Matthews, R. G.; Wolf, S. G.; Yates, J. R.; Pypaert, M.; Horwich, A. L. *Proceedings of the National Academy of Sciences of the United States of America* **2006**, *103*, 15800.
20. Endo, A.; Kurusu, Y. *Biosci Biotechnol Biochem* **2007**, *71*, 1073.
21. Kerner, M. J.; Naylor, D. J.; Ishihama, Y.; Maier, T.; Chang, H. C.; Stines, A. P.; Georgopoulos, C.; Frishman, D.; Hayer-Hartl, M.; Mann, M.; Hartl, F. U. *Cell* **2005**, *122*, 209.
22. Fujiwara, K.; Ishihama, Y.; Nakahigashi, K.; Soga, T.; Taguchi, H. *EMBO J* **2010**, *29*, 1552.
23. Christensen, J. H.; Nielsen, M. N.; Hansen, J.; Fuchtbauer, A.; Fuchtbauer, E. M.; West, M.; Corydon, T. J.; Gregersen, N.; Bross, P. *Cell stress & chaperones* **2010**, *15*, 851.
24. Braig, K.; Otwinowski, Z.; Hegde, R.; Boisvert, D. C.; Joachimiak, A.; Horwich, A. L.; Sigler, P. B. *Nature* **1994**, *371*, 578.
25. Horwich, A. L.; Farr, G. W.; Fenton, W. A. *Chemical reviews* **2006**, *106*, 1917.
26. Sigler, P. B.; Xu, Z. H.; Rye, H. S.; Burston, S. G.; Fenton, W. A.; Horwich, A. L. *Annu Rev Biochem* **1998**, *67*, 581.
27. Fenton, W. A.; Kashi, Y.; Furtak, K.; Horwich, A. L. *Nature* **1994**, *371*, 614.
28. Fenton, W. A.; Horwich, A. L. *Protein science : a publication of the Protein Society* **1997**, *6*, 743.
29. Horwich, A. L.; Low, K. B.; Fenton, W. A.; Hirshfield, I. N.; Furtak, K. *Cell* **1993**, *74*, 909.
30. Horwich, A. L.; Fenton, W. A.; Chapman, E.; Farr, G. W. *Annual review of cell and developmental biology* **2007**, *23*, 115.

31. Saibil, H. R.; Fenton, W. A.; Clare, D. K.; Horwich, A. L. *J Mol Biol* **2013**, *425*, 1476.
32. Nielsen, K. L.; McLennan, N.; Masters, M.; Cowan, N. J. *Journal of bacteriology* **1999**, *181*, 5871.
33. Nielsen, K. L.; Cowan, N. J. *Molecular cell* **1998**, *2*, 93.
34. Illingworth, M.; Ramsey, A.; Zheng, Z. D.; Chen, L. L. *Journal of Biological Chemistry* **2011**, *286*, 30401.
35. Chapman, E.; Farr, G. W.; Fenton, W. A.; Johnson, S. M.; Horwich, A. L. *Proceedings of the National Academy of Sciences of the United States of America* **2008**, *105*, 19205.
36. Chapman, E.; Farr, G. W.; Furtak, K.; Horwich, A. L. *Bioorganic & medicinal chemistry letters* **2009**, *19*, 811.
37. Johnson, S. M.; Sharif, O.; Mak, P. A.; Wang, H. T.; Engels, I. H.; Brinker, A.; Schultz, P. G.; Horwich, A. L.; Chapman, E. *Bioorganic & medicinal chemistry letters* **2014**, *24*, 786.
38. Aza, A.; Unger, R.; Horovitz, A. *FEBS J* **2012**, *279*, 543.
39. Fenton, W. A.; Horwich, A. L. *Quarterly reviews of biophysics* **2003**, *36*, 229.
40. Karplus, M.; Gao, Y. Q.; Ma, J.; van der Vaart, A.; Yang, W. *Philos Trans A Math Phys Eng Sci* **2005**, *363*, 331.
41. Rye, H. S.; Burston, S. G.; Fenton, W. A.; Beechem, J. M.; Xu, Z. H.; Sigler, P. B.; Horwich, A. L. *Nature* **1997**, *388*, 792.
42. Weissman, J. S.; Hohl, C. M.; Kovalenko, O.; Kashi, Y.; Chen, S.; Braig, K.; Saibil, H. R.; Fenton, W. A.; Horwich, A. L. *Cell* **1995**, *83*, 577.
43. Weissman, J. S.; Rye, H. S.; Fenton, W. A.; Beechem, J. M.; Horwich, A. L. *Cell* **1996**, *84*, 481.
44. HayerHartl, M. K.; Weber, F.; Hartl, F. U. *Embo Journal* **1996**, *15*, 6111.
45. Tikhonova, E. B.; Zgurskaya, H. I. *The Journal of biological chemistry* **2004**, *279*, 32116.
46. Yu, E. W.; McDermott, G.; Zgurskaya, H. I.; Nikaido, H.; Koshland, D. E., Jr. *Science* **2003**, *300*, 976.
47. Nishino, K.; Yamaguchi, A. *Journal of bacteriology* **2001**, *183*, 5803.
48. Nishino, K.; Nikaido, E.; Yamaguchi, A. *Biochim Biophys Acta* **2009**, *1794*, 834.
49. Sun, J.; Deng, Z.; Yan, A. *Biochem Biophys Res Commun* **2014**, *453*, 254.
50. Paulsen, I. T.; Sliwinski, M. K.; Saier, M. H., Jr. *J Mol Biol* **1998**, *277*, 573.
51. Galloway, S. M.; Raetz, C. R. *The Journal of biological chemistry* **1990**, *265*, 6394.
52. Vuorio, R.; Vaara, M. *Antimicrob Agents Chemother* **1992**, *36*, 826.
53. Sykes, M. L.; Baell, J. B.; Kaiser, M.; Chatelain, E.; Moawad, S. R.; Ganame, D.; Ioset, J. R.; Avery, V. M. *PLoS Negl Trop Dis* **2012**, *6*, e1896.
54. Sykes, M. L.; Avery, V. M. *Am J Trop Med Hyg* **2009**, *81*, 665.

GroEL/ES inhibitors as potential antibiotics

Supporting Information

Sanofar Abdeen, Nilshad Salim, Najiba Mammadova, Corey Summers, Rochelle Frankson,
Andrew J. Ambrose, Gregory G. Anderson, Peter G. Schultz, Arthur L. Horwich, Eli Chapman,
and Steven M. Johnson*

*To whom correspondence should be addressed:

Tel: 317-274-2458

E-mail: johnstm@iu.edu

Table of Contents:

	<u>Page</u>
Table S1: Comparison of ESKAPE pathogen GroEL and GroES sequence identities.....	S3
Table S2: <i>E. coli</i> GroEL/ES biochemical inhibition results.....	S4
Table S3: <i>E. coli</i> and <i>B. subtilis</i> bacterial proliferation inhibition results.....	S5
Table S4: Inhibition results for GroEL/ES inhibitors against the <i>ESKAPE</i> pathogens	S6
Table S5: HSP60/10 biochemical inhibition and liver and kidney cytotoxicity results.....	S7
Figure S1: Evaluation of bacteriostatic vs. bactericidal mechanisms of action	S8
General Materials and Methods.....	S9
Statistical considerations	S9
Protein expression and purification	S9
Evaluation of compounds in GroEL/ES and HSP60/10-mediated dMDH refolding assays....	S10
Counter-screening compounds for inhibition of native MDH enzymatic activity.....	S10
Evaluation of compounds for inhibition of chaperonin-dependent ATPase activity	S11
Evaluation of compounds in GroEL/ES-mediated dRho refolding assays.....	S11
Counter-screening compounds for inhibition of native Rho enzymatic activity.....	S12
Evaluation of compounds for inhibition of bacterial cell proliferation	S12
Evaluation of bacteriostatic vs. bactericidal mechanisms of action	S13
Evaluation of compounds for cytotoxicity to HEK 293 and THLE-3 cells.....	S14
General Synthetic Methods.....	S14
Compound Syntheses.....	S15-S18
Table S6: Compound characterization data.....	S19
References.....	S20

Table S1: Amino acid sequence conservation for ESKAPE pathogen and human chaperonins and co-chaperonins. Values represent % identical amino conservation compared to *E. coli* GroEL and GroES.

	GroEL (HSP60)	GroES (HSP10)
<i>E. coli</i>	100%	100%
<i>E. faecium</i>	56.5%	47.3%
<i>S. aureus</i>	57.1%	44.1%
<i>K. pneumoniae</i>	96.5%	93.8%
<i>A. baumannii</i>	75.5%	62.1%
<i>P. aeruginosa</i>	80.0%	60.4%
<i>E. cloacae</i>	96.3%	93.8%
<i>H. sapiens</i>	48.0%	35.4%

Table S2: Biochemical inhibition results for *E. coli* GroEL/ES inhibitors. Statistical analyses (two-tailed t-tests) were performed for compound log(IC₅₀) values determined from the GroEL/ES-dRho and GroEL/ES-dMDH refolding assays. Compounds for which there is a statistically significant difference between inhibition results have been marked with a “★” between the two assay results being compared (p < 0.05). P-values could not be calculated for compounds marked with a “#” as one IC₅₀ is greater than the maximum compound concentration tested. For most compounds, IC₅₀ values are not statistically different (17/22 compounds). IC₅₀ correlations are represented graphically in **Figure 3** in the main text.

Biochemical Assay log(IC ₅₀ /μM) Values ± SD						
#	Native Rho Reporter Activity	Native MDH Reporter Activity	GroEL/ES-dRho Refolding	GroEL/ES-dMDH Refolding	GroEL/ES-dMDH ATPase	
1	>2	>1.8	1.47 ± 0.35	★	0.88 ± 0.61	2.08 ± 0.07
5	1.16 ± 0.28	>1.8	-0.23 ± 0.12		-0.16 ± 0.35	>2.4
8	>2	0.85 ± 0.33	0.16 ± 0.06		0.15 ± 0.20	>2.4
9	>2	>1.8	0.14 ± 0.11		-0.03 ± 0.27	1.90 ± 0.07
10	-0.60 ± 0.03	1.73 ± 0.08	-0.33 ± 0.19		-0.10 ± 0.21	2.24 ± 0.05
11	1.06 ± 0.17	>1.8	-0.08 ± 0.04		0.09 ± 0.50	2.34 ± 0.13
14	0.40 ± 0.32	>1.8	0.40 ± 0.31		0.48 ± 0.57	>2.4
15	1.36 ± 0.12	>1.8	0.24 ± 0.14		0.44 ± 0.52	>2.4
18	>2	>1.8	0.83 ± 0.31		0.76 ± 0.29	>2.4
19	0.91 ± 0.30	>1.8	0.48 ± 0.22		0.68 ± 0.48	>2.4
20	>2	>1.8	1.34 ± 0.10	★	0.73 ± 0.26	>2.4
23	0.31 ± 0.17	>1.8	0.38 ± 0.11		0.67 ± 0.82	>2.4
24	>2	>1.8	0.37 ± 0.12		0.56 ± 0.45	>2.4
25	0.16 ± 0.14	>1.8	0.41 ± 0.16		0.81 ± 0.46	>2.4
27	1.09 ± 0.07	>1.8	0.98 ± 0.09	★	0.67 ± 0.30	>2.4
28	0.73 ± 0.54	>1.8	-0.05 ± 0.15		0.42 ± 0.62	>2.4
29	>2	>1.8	1.44 ± 0.13		1.38 ± 0.07	2.27 ± 0.06
31	1.72 ± 0.21	>1.8	1.27 ± 0.14		1.49 ± 0.61	>2.4
32	1.00 ± 0.55	>1.8	1.04 ± 0.32	★	1.62 ± 0.16	2.34 ± 0.04
33	>2	>1.8	>2.4		>2	>2.4
34	>2	>1.8	1.40 ± 0.10		1.38 ± 0.37	>2.4
35	>2	>1.8	1.90 ± 0.34	#	>2	2.03 ± 0.04

IC₅₀ = Inhibitor Concentration resulting in 50% reduction of biochemical activity

Table S3: *E. coli* and *B. subtilis* bacterial proliferation inhibition results for GroEL/ES inhibitors. Results are presented as log(EC₅₀ /μM) values ± their standard deviations (SD).

Bacterial Proliferation log(EC ₅₀ /μM) Values				
#	DH5α <i>E. coli</i>	MC4100 Δ <i>AcrB</i> <i>E. coli</i>	SM101 <i>E. coli</i>	<i>B. subtilis</i>
1	>2	>2	>2	>2
5	>2	1.96 ± 0.10	1.42 ± 0.16	1.40 ± 0.23
8	>2	0.37 ± 0.38	-0.48 ± 0.78	-0.99 ± 0.25
9	>2	>2	1.88 ± 0.12	>2
10	>2	>2	>2	>2
11	>2	>2	1.68 ± 0.31	>2
14	>2	>2	>2	>2
15	>2	>2	1.92 ± 0.09	>2
18	>2	1.32 ± 0.37	0.51 ± 0.25	-0.32 ± 0.34
19	>2	>2	0.88 ± 0.49	1.21 ± 0.46
20	>2	>2	>2	0.45 ± 0.33
23	>2	>2	>2	>2
24	>2	>2	>2	>2
25	>2	>2	>2	>2
27	>2	>2	>2	>2
28	>2	>2	>2	1.63 ± 0.32
29	>2	>2	>2	>2
31	>2	>2	1.27 ± 0.58	1.92 ± 0.09
32	>2	>2	1.83 ± 0.18	1.86 ± 0.07
33	>2	>2	>2	>2
34	>2	>2	1.40 ± 0.23	1.10 ± 0.06
35	>2	>2	>2	>2

EC₅₀ = Effective Concentration of compound resulting in 50% reduction of bacterial proliferation

Table S4: Inhibition results for GroEL/ES inhibitors against the *ESKAPE* pathogens.

#	Bacterial Proliferation log(EC ₅₀ /μM) Values ± SD						
	<i>E. faecium</i>	<i>S. aureus</i>	<i>MRSA</i>	<i>K. pneumoniae</i>	<i>A. baumannii</i>	<i>P. aeruginosa</i>	<i>E. cloacae</i>
1	>2	>2	>2	>2	>2	>2	>2
5	1.96 ± 0.04	1.13 ± 0.24	0.96 ± 0.13	>2	1.76 ± 0.16	>2	>2
8	-0.82 ± 0.10	-0.69 ± 0.20	-0.88 ± 0.13	>2	1.47 ± 0.50	>2	>2
9	>2	>2	>2	>2	>2	>2	>2
10	>2	1.91 ± 0.16	>2	>2	>2	>2	>2
11	>2	1.36 ± 0.29	1.60 ± 0.30	>2	>2	>2	>2
14	>2	>2	1.97 ± 0.06	>2	>2	>2	>2
15	>2	>2	>2	>2	1.91 ± 0.11	>2	>2
18	>2	0.25 ± 0.25	0.12 ± 0.28	>2	>2	>2	>2
19	>2	1.12 ± 0.30	0.17 ± 0.31	>2	>2	>2	>2
20	>2	>2	1.33 ± 0.12	>2	>2	>2	>2
23	>2	>2	>2	>2	>2	>2	>2
24	>2	>2	1.79 ± 0.08	>2	>2	>2	>2
25	>2	>2	>2	>2	>2	>2	>2
27	>2	1.90 ± 0.08	>2	>2	>2	>2	>2
28	>2	1.65 ± 0.13	1.87 ± 0.05	>2	>2	>2	>2
29	>2	>2	1.19 ± 0.15	>2	>2	1.93 ± 0.09	>2
31	>2	>2	1.75 ± 0.20	1.98 ± 0.03	1.50 ± 0.28	>2	>2
32	1.16 ± 0.09	1.92 ± 0.13	1.73 ± 0.11	>2	>2	>2	>2
33	>2	>2	>2	>2	>2	>2	>2
34	>2	>2	>2	>2	>2	>2	>2
35	>2	>2	>2	>2	>2	>2	>2
Ampicillin	-0.20 ± 0.06	-1.23 ± 0.25	1.88 ± 0.08	1.95 ± 0.01	0.41 ± 0.37	1.44 ± 0.01	>2
Minocycline	<-1.3	<-1.3	-0.46 ± 0.06	-0.15 ± 0.25	<-1.3	0.38 ± 0.22	0.17 ± 0.29
Rifampicin	0.08 ± 0.13	<-1.3	-0.81 ± 0.09	0.73 ± 0.08	-0.33 ± 0.26	0.71 ± 0.15	0.79 ± 0.08
Chloramphenicol	0.32 ± 0.03	0.35 ± 0.15	0.37 ± 0.09	0.13 ± 0.12	1.81 ± 0.17	1.21 ± 0.06	0.34 ± 0.08
Kanamycin	>2	0.91 ± 0.18	>2	1.65 ± 0.15	1.20 ± 0.41	1.39 ± 0.24	1.56 ± 0.06
Streptomycin	1.70 ± 0.22	0.56 ± 0.40	>2	0.53 ± 0.58	>2	0.47 ± 0.31	>2
Vancomycin	-0.52 ± 0.07	-0.69 ± 0.15	-0.76 ± 0.05	>2	1.23 ± 0.18	1.87 ± 0.19	>2
Daptomycin	1.51 ± 0.01	0.76 ± 0.28	0.76 ± 0.27	>2	>2	>2	>2

EC₅₀ = Effective Concentration of compound resulting in 50% reduction of bacterial proliferation

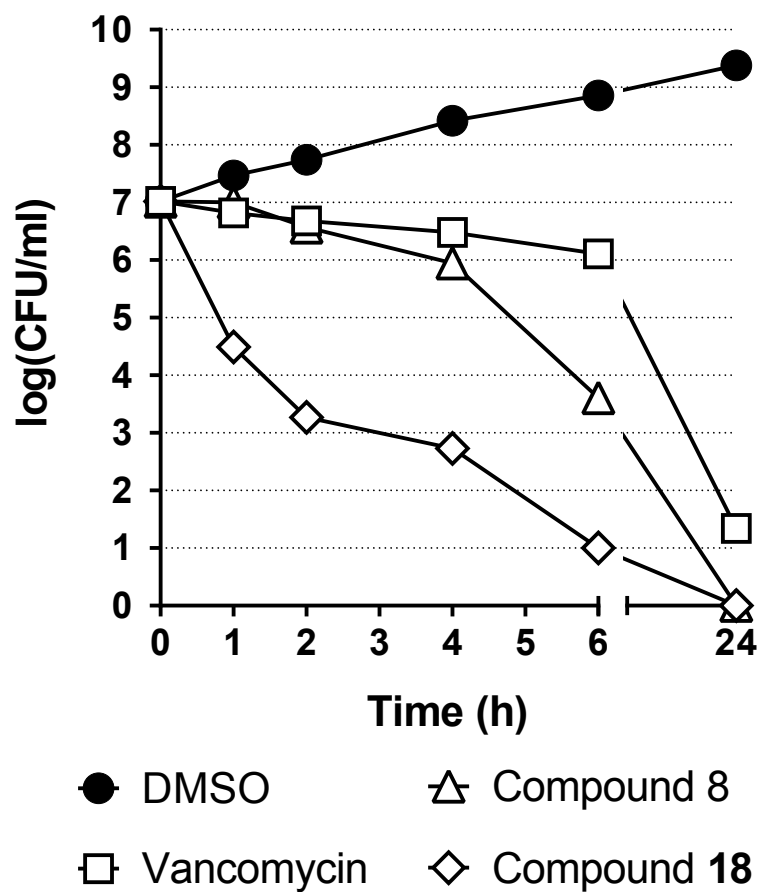
Table S5: Human HSP60/10 biochemical inhibition and liver and kidney cytotoxicity results for the GroEL/ES inhibitors. Statistical analyses (two-tailed t-tests) were performed for compound $\log(\text{IC}_{50})$ values determined from the GroEL/ES-dMDH and HSP60/10-dMDH refolding assays. Compounds for which there is a statistically significant difference between inhibition results have been marked with a “★” between the two assay results being compared ($p < 0.05$). P-values could not be calculated for compounds marked with a “#” as one IC_{50} is greater than the maximum compound concentration tested. IC_{50} correlations are represented graphically in **Figure 5A** in the main text.

#	Biochemical Assay $\log(\text{IC}_{50} / \mu\text{M})$ Values \pm SD			Human Cell Viability Assay $\log(\text{EC}_{50} / \mu\text{M})$ Values \pm SD	
	GroEL/ES-dMDH Refolding	HSP60/10-dMDH Refolding	HSP60/10-dMDH ATPase	THLE-3 (Liver)	HEK 293 (Kidney)
1	0.88 \pm 0.61	★ 1.95 \pm 0.08	2.02 \pm 0.16	1.47 \pm 0.25	1.53 \pm 0.24
5	-0.16 \pm 0.35	★ 0.69 \pm 0.59	>2.4	1.20 \pm 0.06	1.35 \pm 0.27
8	0.15 \pm 0.20	★ 0.74 \pm 0.44	0.55 \pm 0.09	1.08 \pm 0.09	1.89 \pm 0.14
9	-0.03 \pm 0.27	0.20 \pm 0.22	>2.4	>2	>2
10	-0.10 \pm 0.21	★ 0.52 \pm 0.04	2.15 \pm 0.28	>2	>2
11	0.09 \pm 0.50	★ 0.71 \pm 0.15	>2.4	0.99 \pm 0.02	1.10 \pm 0.10
14	0.48 \pm 0.57	0.87 \pm 0.15	>2.4	>2	>2
15	0.44 \pm 0.52	1.01 \pm 0.22	>2.4	>2	1.99 \pm 0.03
18	0.76 \pm 0.29	# >2	>2.4	>2	>2
19	0.68 \pm 0.48	1.20 \pm 0.27	>2.4	1.62 \pm 0.10	1.64 \pm 0.03
20	0.73 \pm 0.26	0.45 \pm 0.54	>2.4	0.56 \pm 0.31	1.23 \pm 0.48
23	0.67 \pm 0.82	1.12 \pm 0.15	>2.4	>2	>2
24	0.56 \pm 0.45	0.91 \pm 0.25	>2.4	1.53 \pm 0.05	1.74 \pm 0.17
25	0.81 \pm 0.46	1.19 \pm 0.11	>2.4	>2	>2
27	0.67 \pm 0.30	★ 1.12 \pm 0.17	>2.4	>2	>2
28	0.42 \pm 0.62	0.26 \pm 0.31	>2.4	>2	>2
29	1.38 \pm 0.07	★ 1.58 \pm 0.18	>2.4	>2	>2
31	1.49 \pm 0.61	# >2	>2.4	1.17 \pm 0.17	0.89 \pm 0.39
32	1.62 \pm 0.16	# >2	>2.4	1.78 \pm 0.11	1.79 \pm 0.16
33	>2	>2	>2.4	>2	>2
34	1.38 \pm 0.37	1.41 \pm 0.53	>2.4	>2	>2
35	>2	>2	>2.4	>2	>2

IC_{50} = Inhibitor Concn IC_{50} = Inhibitor Concentration resulting in 50% reduction of biochemical activity

EC_{50} = Effective Concn EC_{50} = Effective Concentration of compound resulting in 50% reduction in cell viability

Figure S1: Evaluation of bacteriostatic vs. bactericidal mechanisms of action. Compounds **8**, **18**, and vancomycin were tested at concentrations of 4x their MICs against *S. aureus* (ATCC 25923). MIC values were determined to be 0.60 μM (0.34 $\mu\text{g}/\text{mL}$) for compound **8**, 8.0 μM (2.4 $\mu\text{g}/\text{mL}$) for compound **18**, and 1.6 μM (2.3 $\mu\text{g}/\text{mL}$) for vancomycin under these experimental conditions. All compounds appear to be bactericidal. Data presented are the averages of triplicate experiments.



General Materials and Methods.

DH5 α and BL21 (DE3) *E. coli* cells were purchased from New England Biolabs, and Rosetta™ 2 (DE3) *E. coli* cells from EMD Millipore. MC4100 Δ *acrB* *E. coli* cells were provided by Prof. Eli Chapman, University of Arizona, College of Pharmacy. *E. coli* SM101 *lpxA2* cells were obtained from the *Coli* Genetic Stock Center at Yale University (CGSC #7255). *B. subtilis* 168 cells were provided by Dr. Leendert Hamoen from the University of Amsterdam, Swammerdam Institute for Life Sciences (SILS). The *ESKAPE* pathogens were purchased from the American Type Culture Collection (ATCC): *E. faecium* (Orla-Jensen) Schleifer and Kilpper-Balz strain NCTC 7171 (ATCC 19434); *S. aureus* subsp. *aureus* Rosenbach strain Seattle 1945 (ATCC 25923); Methicillin-resistant *S. aureus* (MRSA) subsp. *aureus* Rosenbach strain HPV107 (ATCC BAA-44); *K. pneumoniae*, subsp. *pneumoniae* (Schroeter) Trevisan strain NCTC 9633 (ATCC 13883); *A. baumannii* Bouvet and Grimont strain 2208 (ATCC 19606); *P. aeruginosa* (Schroeter) Migula strain NCTC 10332 (ATCC 10145); *E. cloacae*, subsp. *cloacae* (Jordan) Hormaeche and Edwards strain CDC 442-68 (ATCC 13047). HEK 293 kidney cells (ATCC CRL-1573) and THLE-3 liver cells (ATCC CRL-11233) were used for compound toxicity assays. Antibiotics were used in following concentrations when appropriate; Kanamycin (34 μ g/mL), Ampicillin (50 μ g/mL), Chloramphenicol (30 μ g/mL) and Streptomycin (100 μ g/mL). Test compounds were purchased from commercial suppliers where available (Chembridge, ChemDiv, Ambinter, Aldrich, Asinex, and Ryan Scientific), or synthesized according to literature procedures (compounds **10**, **15**, **23**, **24**, and **25** – synthetic protocols are presented in the Supplementary Data below). Compounds **2-4**, **6**, **7**, **12**, **13**, **16**, **17**, **21**, **22**, **26**, **30**, and **36** were omitted from evaluation as they were either not commercially available, or purchased compounds were not readily identified by LC-MS and/or did not have acceptable purities confirmed by HPLC. For ease of comparison, compound numbering from **1-36** was maintained as presented in our previous high-throughput screening study.¹

Statistical considerations.

All IC₅₀ (or EC₅₀) values reported are averages of IC₅₀ (or EC₅₀) values determined from individual dose-response curves in replicate assays as follows: 1) Individual IC₅₀ values from replicate assays were first log-transformed and the average log(I/EC₅₀) values and standard deviations (SD) calculated; 2) Replicate log(I/EC₅₀) values were evaluated for outliers using the ROUT method in GraphPad Prism 6 (Q of 10%); 3) Average IC₅₀ (or EC₅₀) values were then back-calculated from the average log(I/EC₅₀) values. To compare statistical differences between log(IC₅₀) values, two-tailed, unpaired t-tests were performed using GraphPad Prism 6 (0.05 alpha level).

Protein Expression and purification.

E. coli GroEL was expressed from a *trc*-promoted plasmid in DH5 α *E. coli* cells and purified as previously reported.¹ *E. coli* GroES was expressed from a *T7*-promoted plasmid in *E. coli* BL21 (DE3) cells and purified as previously reported.¹ Human HSP60 was expressed from a *T7*-promoted plasmid in Rosetta™ 2 (DE3) *E. coli* cells and purified as previously reported.² For human HSP10 purification, pET30-*HSP10* was transformed into Rosetta™ 2 (DE3) *E. coli* cells for over-expression. Cells were grown at 37°C in LB/Kanamycin/Chloramphenicol medium until an OD₆₀₀ of 0.5 was reached, then were induced with 0.5 mM IPTG and continued to grow for 2-3 h at 37°C. The culture was centrifuged at 14,000 rpm, and the cell pellet was re-suspended in Buffer A (50 mM sodium acetate, pH 4.5, and 0.5 mM EDTA), supplemented with EDTA-free complete protease inhibitor cocktail (Roche), 100 μ g/ml lysozyme, 10 μ L (1000 u/ml) DNAase, and lysed by sonication. Clarified cell lysate was loaded on a cation exchange column (SP Sepharose fast flow resin, GE) and eluted with linear NaCl gradient with Buffer B (sodium acetate, pH 4.5, 0.5 mM EDTA, and 1 M NaCl). Fractions containing HSP10 were concentrated, dialyzed with storage buffer (50 mM Tris-HCl, pH 7.4, and 300 mM NaCl) using 10 kDa SnakeSkin™ dialysis tubing (Thermo Scientific) and re-purified on a Superdex 200 column (HiLoad 26/600, GE) in storage buffer. The concentration of protein was determined by Coomassie Protein

Assay Kit (Thermo Scientific). Protein was stored at 4°C in 50 mM Tris-HCl, pH 7.4, 300 mM NaCl, and 1 mM DTT.

Evaluation of compounds in GroEL/ES and HSP60/10-mediated dMDH refolding assays.

Reagent preparation: For these assays, four primary reagent stocks were prepared: 1) GroEL/ES-dMDH or HSP60/10-dMDH binary complex stock; 2) ATP initiation stock; 3) EDTA quench stock; 4) MDH enzymatic assay stock. Denatured MDH (dMDH) was prepared by 2-fold dilution of MDH (5 mg/ml, soluble pig heart MDH from Roche, product #10127248001) with denaturant buffer (7 M guanidine-HCl, 200 mM Tris, pH 7.4, and 50 mM DTT). MDH was completely denatured by incubating at room temperature for 30 min. The binary complex solutions were prepared by slowly adding the dMDH stock to a stirring stock with GroEL (or HSP60) in folding buffer (50 mM Tris-HCl, pH 7.4, 50 mM KCl, 10 mM MgCl₂, and 1 mM DTT), followed by addition of GroES (or HSP10). The binary complex stocks were prepared immediately prior to use and had final protein concentrations of 83.3 nM GroEL (*Mr* 800 kDa) or HSP60 (*Mr* 400 kDa), 100 nM GroES or HSP10 (*Mr* 70 kDa), and 20 nM dMDH in folding buffer. For the ATP initiation stock, ATP solid was diluted into folding buffer to a final concentration of 2.5 mM. Quench solution contained 600 mM EDTA (pH 8.0). The MDH enzymatic assay stock consisted of 20 mM sodium mesoxalate and 2.4 mM NADH in reaction buffer (50 mM Tris-HCl, pH 7.4, 50 mM KCl, and 1 mM DTT).

Assay Protocol: First, 30 µL aliquots of the GroEL/ES-dMDH or HSP60/10-dMDH binary complex stocks were dispensed into clear, 384-well polystyrene plates. Next, 0.5 µL of the compound stocks (10 mM to 4.6 µM, 3-fold dilutions in DMSO) were added by pin-transfer (V&P Scientific). The chaperonin-mediated refolding cycles were initiated by addition of 20 µL of ATP stock (reagent concentrations during refolding cycle: 50 nM GroEL or HSP60, 60 nM GroES or HSP10, 12 nM dMDH, 1 mM ATP, and compounds of 100 µM to 46 nM, 3-fold dilution series). After incubation for 60 minutes at 37°C, the assays were quenched by addition of 10 µL of the EDTA to final concentration of 100 mM. Enzymatic activity of the refolded MDH was initiated by addition of 20 µL MDH enzymatic assay stock (20 mM sodium mesoxalate and 2.4 mM NADH in reaction buffer, 50 mM Tris pH 7.4, 50 mM KCl, 1 mM DTT), and followed by measuring the NADH absorbance in each well at 340 nm using a Molecular Devices, SpectraMax Plus384 microplate reader (NADH absorbs at 340 nm, while NAD⁺ does not). A₃₄₀ measurements recorded at 0.5 minutes (start point) and at successive time points until the amount of NADH consumed reached ~90% (end point, generally between 30-60 minutes). The differences between the start and end point A₃₄₀ values were used to calculate the % inhibition of the GroEL/ES or HSP60/10 machinery by the compounds. IC₅₀ values for the test compounds were obtained by plotting the % inhibition results in GraphPad Prism 6 and analyzing by non-linear regression using the log (inhibitor) vs. response (variable slope) equation. Results presented represent the averages of IC₅₀ values obtained from at least triplicate experiments.

Counter-screening compounds for inhibition of native MDH enzymatic activity.

Reagent Preparations & Assay Protocol: Reagents were identical to those used in the GroEL/ES-dMDH refolding assay described above; however, the assay protocol differed in the sequence of compound addition to the wells. Compounds were pin-transferred after the EDTA quenching step, but prior to the addition of the enzymatic reporter reagents. Thus, the refolding reactions were allowed to proceed for 60 min at 37°C in the absence of test compounds, but the enzymatic activity of the refolded MDH reporter enzyme was monitored in the presence of test compounds (inhibitor concentration range during the enzymatic reporter reaction is 83.3 µM to 38 nM – 3-fold dilutions). IC₅₀ values for the MDH reporter enzyme were determined as described above. Results presented represent the averages of IC₅₀ values obtained from at least triplicate experiments.

Evaluation of compounds for inhibition of chaperonin-dependent ATPase activity.

Reagent preparation: For these assays, four primary reagent stocks were prepared: 1) GroEL/ES-dMDH or human HSP60/10-dMDH binary complex stock; 2) ATP initiation stock; 3) EDTA quench stock; 4) malachite green reporter stock. The dMDH stock was prepared as in the above refolding assays. Binary complex solutions were immediately prepared prior to use, with final concentrations of 100 nM GroEL or HSP60, 120 nM GroES or HSP10, and 250 nM dMDH in folding buffer (50 mM Tris-HCl, pH 7.4, 50 mM KCl, 10 mM MgCl₂, and 1 mM DTT). For the ATP initiation stock, ATP solid was diluted into folding buffer to a final concentration of 2 mM. Quench solution contained 300 mM EDTA (pH 8.0). The malachite green reporter stock consisted of 0.034% malachite green and 1.04% ammonium molybdate tetrahydrate in 1 M HCl with 0.02% Tween-20.

Assay protocol: First, 10 μ L aliquots of binary stock were dispensed into clear, flat-bottom, 384-well polystyrene plates. Next, 0.5 μ L of the compound stocks (10 mM to 4.6 μ M, 3-fold dilutions in DMSO) were added by pin-transfer. The ATP-dependent chaperonin refolding cycles were initiated by addition of 10 μ L ATP stock (reagent concentrations during the assay; 50 nM GroEL or HSP60, 60 nM GroES or HSP10, 125 nM dMDH, 1 mM ATP, and compounds from 250 μ M to 114 nM, 3-fold dilution series). The reactions were incubated at 37°C for 60 minutes, then were quenched by addition of 10 μ L of the EDTA solution. After quenching, 60 μ L of the malachite green reporter stock was added and incubated at room temperature for 15 min, then the absorption was measured at 600 nm. A second set of baseline control plates were prepared analogously, but without binary solution, to correct for possible interference from compound absorbance or turbidity. IC₅₀ values for the test compounds were obtained by plotting the OD₆₀₀ results in GraphPad Prism 6 and analyzing by non-linear regression using the log(inhibitor) vs. response (variable slope) equation. Results presented represent the averages of IC₅₀ values obtained from at least triplicate experiments.

Evaluation of compounds in GroEL/ES in denatured Rhodanese refolding assay.

Reagent preparation: For this assay, five primary reagent stocks were prepared: 1) GroEL/ES-dRho binary complex stock; 2) ATP initiation stock; 3) thiocyanate enzymatic assay stock; 4) formaldehyde quench stock; 5) ferric nitrate reporter stock. Denatured Rhodanese (dRho) was prepared by 3-fold dilution of Rhodanese (Roche product #R1756, diluted to 10 mg/mL with H₂O) with denaturant buffer (12 M Urea, 50 mM Tris-HCl, pH 7.4, and 10 mM DTT). Rhodanese was completely denatured by incubating at room temperature for 30 min. The binary complex solution was prepared by slowly adding the dRho stock to a stirring stock of concentrated GroEL in modified folding buffer (50 mM Tris-HCl, pH 7.4, 50 mM KCl, 10 mM MgCl₂, 5 mM Na₂S₂O₃ and 1 mM DTT). The solution was centrifuged at 16,000 x g for 5 minutes, and the supernatant was collected and added to a solution of GroES in modified folding buffer to give final protein concentrations of 100 nM GroEL, 120 nM GroES, and 80 nM dRho in modified folding buffer. The binary complex stock was prepared immediately prior to use. For the ATP initiation stock, ATP solid was diluted into modified folding buffer to a final concentration of 2.0 mM. The thiocyanate enzymatic assay stock was prepared to contain 70 mM KH₂PO₄, 80 mM KCN, and 80 mM Na₂S₂O₃ in water. The formaldehyde quench solution contained 30% formaldehyde in water. The ferric nitrate reporter stock contained 8.5% w/v Fe(NO₃)₃ and 11.3% v/v HNO₃ in water.

Assay Protocol: First, 10 μ L aliquots of the GroEL/ES-dRho complex stock was dispensed into clear, 384-well polystyrene plates. Next, 0.5 μ L of the compound stocks (10 mM to 4.6 μ M, 3-fold dilutions in DMSO) were added by pin-transfer. The chaperonin-mediated refolding cycle was initiated by addition of 10 μ L of ATP stock (reagent concentrations during refolding cycle: 50 nM GroEL, 60 nM GroES, 40 nM dRho, 1 mM ATP, and compounds of 250 μ M to 114 nM, 3-fold dilution series). After incubating for 60 minutes at 37°C for the refolding cycle, 30 μ L of the thiocyanate enzymatic assay

stock was added and incubated for 60 min at R.T. for the refolded Rhodenase enzymatic reporter reaction. The reporter reaction was quenched by adding 10 μ L of the formaldehyde quench stock, and then 40 μ L of the ferric nitrate reporter stock was added to quantify the amount of thiocyanate produced during the enzymatic reporter reaction, which is proportional to the amount of dRho refolded by GroEL/ES. After incubating at R.T. for 15 min, the absorbance by Fe(SCN)₃ was measured at 460 nm using a Molecular Devices, SpectraMax Plus384 microplate reader. A second set of baseline control plates were prepared analogously, but without binary solution, to correct for possible interference from compound absorbance or turbidity. IC₅₀ values for the test compounds were obtained by plotting the A₄₆₀ results in GraphPad Prism 6 and analyzing by non-linear regression using the log(inhibitor) vs. response (variable slope) equation. Results presented represent the averages of IC₅₀ values obtained from at least triplicate experiments.

Counter-screening compounds for inhibition of native Rhodanese enzymatic activity.

Reagent Preparations & Assay Protocol: Reagents were identical to those used in the GroEL/ES-dRho refolding assay described above; however, the assay protocol differed in the sequence of compound addition to the wells. Compounds were pin-transferred after the incubation for 60 minutes at 37°C for the refolding cycle, but prior to the addition of the thiocyanate enzymatic assay stock. Thus, the refolding reactions were allowed to proceed for 60 min at 37°C in the absence of test compounds, but the enzymatic activity of the refolded Rhodanese reporter enzyme was monitored in the presence of test compounds (inhibitor concentration range during the enzymatic reporter reaction is 100 μ M to 46 nM – 3-fold dilutions). IC₅₀ values for the Rhodenase reporter enzyme were determined as described above. Results presented represent the averages of IC₅₀ values obtained from at least triplicate experiments.

Evaluation of compounds for inhibition of bacterial cell proliferation.

All *E.coli* strains and *B. subtilis* 168 were grown using Luria-Bertani (LB) media broth/agar, unless specified otherwise. *S. aureus* and MRSA were grown using ATCC Medium 18. All other *ESKAPE* pathogens (*E. faecium*, *K. pneumonia*, *A. baumannii*, *P. aeruginosa*, and *E. cloacae*), were grown using Brain Heart Infusion media broth/agar (Becton, Dickinson and Company).

General Assay Protocol: Stock bacterial cultures were streaked onto agar plates and grown overnight at 37°C. Fresh aliquots of broth were inoculated with single bacterial colonies and the cultures were grown overnight at 37°C with shaking (250 rpm). The following morning, the overnight cultures were sub-cultured (1:5 dilution) into fresh aliquots of media and grown at 37°C for 2 h with shaking. After 2 h, cultures were diluted into fresh media to achieve final OD₆₀₀ readings of 0.0125. Aliquots of these diluted cultures (80 μ L) were added to clear, flat-bottom, 384-well polystyrene plates that were stamped with 1.0 μ L of test compounds in 20 μ L media (8x, 3-fold dilution series stocks ranging from 10 mM to 4.6 μ M in DMSO). Plates were sealed with "Breathe Easy" oxygen permeable membranes (Diversified Biotech) and left to incubate at 37°C without shaking (stagnant assay). OD₆₀₀ readings were taken at the 6-8 h time points, depending on the time for each bacterial strain to reach mid-log phase growth. A second set of baseline control plates were prepared analogously, but without any bacteria added, to correct for possible compound absorbance and/or precipitation. EC₅₀ values for the test compounds were obtained by plotting the OD₆₀₀ results in GraphPad Prism 6 and analyzing by non-linear regression using the log(inhibitor) vs. response (variable slope) equation. Results presented represent the averages of EC₅₀ values obtained from at least triplicate experiments.

Evaluation of compounds for inhibition of MC4100 Δ acrB *E. coli* cell growth: MC4100 Δ acrB *E. coli* were streaked onto an LB agar plate containing 50 μ g/mL kanamycin and grown overnight at 37°C. The following morning, the overnight culture was sub-cultured (1:5 dilution) into a fresh aliquot of media, without addition of antibiotic, and grown at 37°C for 2 h with shaking. After 2 h, the culture was diluted

into fresh media to achieve a final OD₆₀₀ reading of 0.0125. All the other steps were followed identically as described above.

Evaluation of compounds for inhibition of SM101 *lpxA2* *E. coli* cell growth:^{3,4} SM101 *lpxA2* *E. coli* were streaked onto an LB agar plate containing 50 µg/mL streptomycin and grown at 31°C. A fresh aliquot of LB media (without any NaCl but with streptomycin added) was inoculated with a single bacterial colony and the culture was split into two, with one half grown overnight at 31°C and the other at 37°C (no growth control), with shaking at 250 rpm. The following morning, the culture grown at 31°C was diluted into fresh LB media to achieve a final OD₆₀₀ reading of 0.0125 (if the culture incubated at 37°C grew, new cultures were prepared). Aliquots of this diluted culture (80 µL) were added to 384-well clear bottom polystyrene plates that had been previously stamped with 1.0 µL of test compounds in 20 µL media (8x, 3-fold dilution series stocks ranging from 10 mM to 4.6 µM in DMSO; compounds were added by pin transfer). The plates were sealed with "Breathe Easy" oxygen permeable membranes and left to incubate at 31°C for 12 h without shaking (stagnant assay). At the 12 h time point, the plates were removed and the OD₆₀₀ read using a SpectraMax Plus 384 UV-Vis spectrophotometer to follow cell growth. A second set of baseline control plates were prepared analogously, but without any bacteria added, to correct for possible compound absorbance and/or precipitation. Separate control cultures were prepared from the diluted SM101 *lpxA2* bacteria and grown at 31°C and 37°C, with shaking at 250 rpm, to verify growth in the 31°C culture and no growth in the 37°C culture. If bacteria grew in the 37°C no growth control, then the assay was repeated. EC₅₀ values were determined as described above. Results presented represent the averages of EC₅₀ values obtained from at least triplicate experiments.

Evaluation of bacteriostatic vs. bactericidal mechanisms of action.

Minimal inhibitory concentration (MIC) determination.

A fresh aliquot of ATCC Medium 18 (Tryptic Soy broth) was inoculated with a single *S. aureus* (ATCC 25923) bacterial colony and the culture was grown overnight at 37°C with shaking (250 rpm). The following morning, the overnight culture was diluted 5-fold into fresh media and grown at 37°C for 1 h with shaking. After 1 h, the sub-culture was diluted to an OD₆₀₀ of 0.01 (~10⁷ CFU/ml) in fresh media. 200 µL aliquots were added to clear, flat-bottom, 96-well polystyrene plates. 2 µL of compounds **8**, **18**, and vancomycin in DMSO were then added to the wells (final concentrations of compounds were: **8** = 0.2, 0.4, 0.6, 0.8, 1.0, and 1.2 µM; **18** = 2, 4, 6, 8, 10, and 12 µM; vancomycin = 1.2, 1.4, 1.6, 1.8, 2.0, and 2.2 µM). The plates were then sealed with "Breathe Easy" oxygen permeable membranes (Diversified Biotech) and incubated at 37°C without shaking (stagnant assay) for 24 h, after which the MICs were identified visually (MICs: **8** = 0.6 µM; **18** = 8 µM; Vancomycin = 1.6 µM).

Bactericidal activity of compounds.

A fresh aliquot of ATCC Medium 18 was inoculated with a single *S. aureus* (ATCC 25923) bacterial colony and the culture was grown overnight at 37°C with shaking (250 rpm). The following morning, the overnight culture was diluted 5-fold into fresh media and grown at 37°C for 1 h with shaking. After 1 h, the sub-culture was diluted to optical density OD₆₀₀ of 0.01 (~10⁷ CFU/ml) in fresh media. Aliquots of these diluted cultures (6 mL) were treated with DMSO (no compound control) or 4x MIC of compounds **8**, **18**, and vancomycin (60 µL of each compound stocks were added to achieve respective 4x MIC, final DMSO concentration in all cultures were maintained at 1%). All cultures were incubated at 37°C with shaking (250 rpm) and viable cell counts were determined at 0, 1, 2, 4, 6, and 24 h time intervals by dilution and plating on ATCC Medium 18 agar. Time-kill curves presented in **Figure S1** are averaged values from triplicate experiments.

Evaluation of compounds for cytotoxicity to HEK 293 and THLE-3 cells.

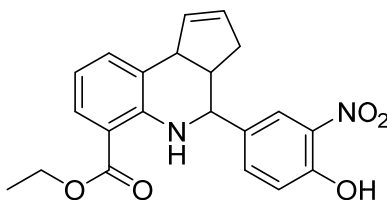
Cell cytotoxicity assays were performed using the Alamar Blue reporter reagents as previously described.^{5,6} HEK 293 cells were maintained in MEM medium (Corning Cellgro, 10-009 CV) supplemented with 10% FBS (Sigma, F2242). THLE-3 cells were maintained in Clonetics BEBM medium (Lonza, CC-3171) supplemented with the BEGM bullet kit (Lonza, CC-3170) and 10% FBS. All assays were carried out in 384-well plates (BRAND cell culture grade plates, 781980). Briefly, cells at 80% confluence were harvested and diluted in growth medium, then 50 μ L of the HEK 293 cells (15,000 cells/well) or THLE-3 cells (5,000 cells/well) were plated and incubated at 37°C with 5% CO₂ for 24 h. Compound stocks (0.5 μ L of 10 mM to 4.6 μ M, 3-fold dilutions in DMSO) were added by pin-transfer and the plates were incubated for an additional 48 h at 37°C with 5% CO₂. The Alamar Blue reporter reagents were then added to a final concentration of 10%. The plates were incubated for 4 h (HEK 293) or 6 h (THLE-3), then sample fluorescence (535 nm excitation, 590 nm emission) was read using a Molecular Devices FlexStation II 384-well plate reader. Cell viability was calculated as per vendor instructions. EC₅₀ values for the test compounds were obtained by plotting the % Alamar Blue reduction results in GraphPad Prism 6 and analyzing by non-linear regression using the log(inhibitor) vs. response (variable slope) equation. Results presented represent the averages of EC₅₀ values obtained from at least triplicate experiments.

General Synthetic Methods.

Test compounds were purchased from commercial suppliers where available (Chembridge, ChemDiv, Ambinter, Aldrich, Asinex, and Ryan Scientific), or synthesized as indicated below for compounds **10**, **15**, **23**, **24**, and **25**. Compounds **2-4**, **6**, **7**, **12**, **13**, **16**, **17**, **21**, **22**, **26**, **30**, and **36** were omitted from evaluation as they were either not commercially available, or purchased compounds were not readily identified by LC-MS and/or acceptable purities confirmed by HPLC. Reaction progress was monitored by thin-layer chromatography on silica gel 60 F254 coated glass plates (EM Sciences). Flash chromatography was performed using a Biotage Isolera One flash chromatography system and eluting through Biotage KP-Sil Zip or Snap silica gel columns. Reverse phase high performance liquid chromatography (RP-HPLC) was performed using a Waters 1525 binary pump, 2489 tunable UV/Vis detector (254 and 280 nm detection), and 2707 autosampler. For analytical HPLC evaluation, samples were chromatographically separated using a Waters XSelect CSH C18 column (part number 186005282, 130 Å pore size, 5 μ m particle size, 3.0x150 mm), eluting with a H₂O:CH₃CN gradient solvent system. Linear gradients were run from either 100:0, 80:20, or 60:40 A:B to 0:100 A:B (A = 95:5 H₂O:CH₃CN, 0.05% TFA; B = 5:95 H₂O:CH₃CN, 0.05% TFA). All test compounds were found to be >95% purity, with exception of the following: **14** = 85%, **19** = 79%, **20** = 92%, **27** = 94%, **28** = 78%, and **34** = 84%. For preparatory HPLC purification, samples were chromatographically separated using a Waters XSelect CSH C18 OBD prep column (part number 186005422, 130 Å pore size, 5 μ m particle size, 19x150 mm) employing the above H₂O:CH₃CN solvent systems. All compounds (purchased or synthesized) were confirmed by mass spectrometry, with data collected using an Agilent analytical LC-MS at the IU Chemical Genomics Core Facility (CGCF). ¹H-NMR spectra were recorded on either a Bruker 300 MHz or Bruker 500 MHz spectrometer. Chemical shifts are reported in parts per million and calibrated to the *d*₆-DMSO solvent peaks at 2.50 ppm.

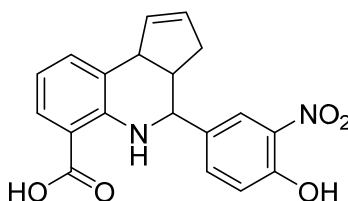
Compound Syntheses.

Ethyl-4-(4-hydroxy-3-nitrophenyl)-3a,4,5,9b-tetrahydro-3H-cyclopenta[c]quinoline-6-carboxylate (37).⁷⁻⁹



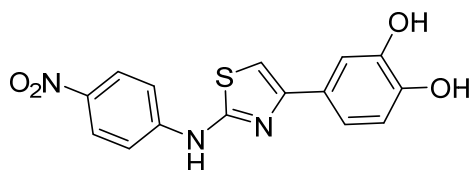
To a stirring mixture of 4-hydroxy-3-nitrobenzaldehyde (289 mg, 1.73 mmol) and ethyl-2-aminobenzoate (0.25 mL, 1.7 mmol) in anhydrous acetonitrile (20 mL) was added TFA (0.12 mL, 1.6 mmol), and the reaction was left to stir for 1 h at R.T. (under Ar). Then, cyclopentadiene was added (0.75 mL, 18 mmol, freshly distilled from dicyclopentadiene) and the reaction was left to stir for 18 h. The reaction was then concentrated and flash chromatographic purification over silica (hexanes:DCM gradient) afforded ethyl-4-(4-hydroxy-3-nitrophenyl)-3a,4,5,9b-tetrahydro-3H-cyclopenta[c]quinoline-6-carboxylate (**37**) as a yellow solid (530 mg, 82%). ¹H-NMR (500 MHz, *d*₆-DMSO) δ 7.92 (d, *J*=2.2 Hz, 1H), 7.66 (dd, *J*=1.1, 8.0 Hz, 1H), 7.57-7.63 (m, 2H), 7.29 (d, *J*=7.3 Hz, 1H), 7.15 (d, *J*=8.8 Hz, 1H), 6.68 (t, *J*=7.7 Hz, 1H), 5.85-5.89 (m, 1H), 5.61 (d, *J*=5.0 Hz, 1H), 4.69 (d, *J*=3.5 Hz, 1H), 4.25 (q, *J*=6.9 Hz, 2H), 4.12 (d, *J*=9.1 Hz, 1H), 2.97-3.05 (m, 1H), 2.33-2.40 (m, 1H), 1.72-1.80 (m, 1H), 1.29 (t, *J*=7.3 Hz, 3H); LC-MS [MH]⁺ expected = 381.2 (C₂₁H₂₁N₂O₅), observed = 381.1; HPLC: 98% pure.

4-(4-Hydroxy-3-nitrophenyl)-3a,4,5,9b-tetrahydro-3H-cyclopenta[c]quinoline-6-carboxylic acid (10).



Compound **37** (153 mg, 0.402 mmol) was stirred with LiOH·H₂O (167 mg, 3.98 mmol) in H₂O/MeOH/THF (1/1/3 mL) at 60°C. After 1 h, the reaction was acidified with 1 M HCl and extracted into EtOAc. The organics were washed with brine, dried over Na₂SO₄, filtered, and concentrated. Prep-HPLC purification afforded 4-(4-hydroxy-3-nitrophenyl)-3a,4,5,9b-tetrahydro-3H-cyclopenta[c]quinoline-6-carboxylic acid (**10**) as a yellow solid (119 mg, 84%). ¹H-NMR (300 MHz, *d*₆-DMSO) δ 7.86-7.963 (m, 2H), 7.64 (d, *J*=6.6 Hz, 2H), 7.25 (d, *J*=6.9 Hz, 1H), 7.19 (d, *J*=8.8 Hz, 1H), 6.64 (t, *J*=7.6 Hz, 1H), 5.87 (br s, 1H), 5.6 (d, *J*=5.4 Hz, 1H), 4.69 (br s, 1H), 4.11 (d, *J*=9.1 Hz, 1H), 2.95-3.05 (m, 1H), 2.33-2.41 (m, 1H); LC-MS [MH]⁺ expected = 353.1 (C₁₉H₁₇N₂O₅), observed = 353.1; HPLC: >99% pure.

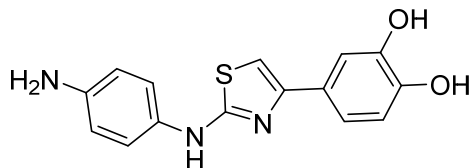
4-(2-((4-Nitrophenyl)amino)thiazol-4-yl)benzene-1,2-diol (38).^{10, 11}



2-Chloro-3',4'-dihydroxyacetophenone (567 mg, 3.04 mmol) and *N*-(4-nitrophenyl)thiourea (555 mg, 2.81 mmol) were refluxed in ethanol (20 mL) for 4 h, then cooled on ice. The precipitate was filtered, rinsed with ice cold EtOH, and dried to afford 4-(2-((4-nitrophenyl)amino)thiazol-4-yl)benzene-1,2-diol

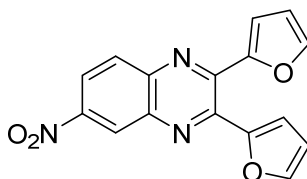
(**38**) as a yellow powder (750 mg, 81%). ¹H-NMR (500 MHz, *d*₆-DMSO) δ 11.04 (s, 1H), 8.25 (d, *J*=9 Hz, 2H), 7.94 (d, *J*=9.1 Hz, 2H), 7.35 (d, *J*=2.2 Hz, 1H), 7.24 (dd, *J*=2.0, 8.0 Hz, 1H), 7.19 (s, 1H), 6.79 (d, *J*=8.2 Hz, 1H); LC-MS [*M*-H]⁻ expected = 328.0 (C₁₅H₁₀N₃O₄S), observed = 327.9; HPLC: 98% pure.

4-(2-((4-Aminophenyl)amino)thiazol-4-yl)benzene-1,2-diol (**15**).



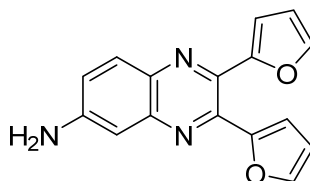
Tin powder (884 mg, 7.45 mmol) was added portion-wise to a stirring mixture of compound **38** (721 mg, 2.41 mmol) in 10% HCl in AcOH (11 mL) and the reaction was stirred at 100°C for 2 h, then at R.T. overnight. The reaction was then diluted into 50% EtOAc in water and neutralized with solid NaHCO₃. The slurry was filtered and the organics collected, dried over Na₂SO₄, filtered, and concentrated. Flash chromatographic purification over silica (hexanes:EtOAc gradient), followed by prep-HPLC purification afforded 4-(2-((4-aminophenyl)amino)thiazol-4-yl)benzene-1,2-diol (**15**) as an off-white solid (21.3 mg, 3%). ¹H-NMR (500 MHz, *d*₆-DMSO) δ 10.31 (s, 1H), 9.06 (br s, 1H), 8.92 (br s, 1H), 7.78 (d, *J*=8.8 Hz, 2H), 7.31 (d, *J*=1.9 Hz, 1H), 7.26 (d, *J*=8.2 Hz, 2H), 7.20 (dd, *J*=2.2, 8.2 Hz, 1H), 7.00 (s, 1H), 6.77 (d, *J*=8.2 Hz, 1H); LC-MS [*M*H]⁺ expected = 300.1 (C₁₅H₁₄N₃O₂S), observed = 300.0; HPLC: 99% pure.

2,3-Di(furan-2-yl)-6-nitroquinoxaline (**39**).¹²⁻¹⁴



1,2-Diamino-4-nitrobenzene (1.57 g, 10.3 mmol) and 2,2'-fural (1.93 g, 10.2 mmol) were refluxed together in EtOH (40 mL) for 4 h. The reaction was then cooled over ice and the precipitate filtered, rinsed with ice-cold EtOH and hexanes, collected, and dried to afford 2,3-di(furan-2-yl)-6-nitroquinoxaline (**39**) as an orange solid (2.54 g, 81%). ¹H-NMR (300 MHz, *d*₆-DMSO) δ 8.84 (d, *J*=2.2 Hz, 1H), 8.51 (dd, *J*=2.6, 9.2 Hz, 1H), 8.28 (d, *J*=9.2 Hz, 1H), 7.97-8.02 (m, 2H), 6.92 (dd, *J*=0.7, 3.4 Hz, 1H), 6.87 (dd, *J*=0.7, 3.5 Hz, 1H), 6.77 (dt, *J*=1.6, 3.4 Hz, 2H); LC-MS [*M*H]⁺ expected = 308.1 (C₁₆H₁₀N₃O₄), observed = 308.0; HPLC: 96% pure.

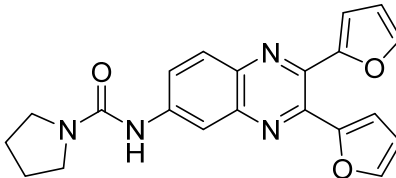
2,3-Di(furan-2-yl)quinoxalin-6-amine (**40**).



Tin powder (2.83 g, 23.8 mmol) was added portion-wise to a stirring mixture of compound **39** (2.40 g, 7.81 mmol) in 10% HCl in AcOH (22 mL) and the reaction was stirred at R.T. overnight. The reaction was then diluted into 50% EtOAc in water and neutralized with solid NaHCO₃. The slurry was filtered and the organics collected, dried over Na₂SO₄, filtered, and concentrated. Flash chromatographic purification over silica (hexanes:EtOAc gradient) afforded 2,3-di(furan-2-yl)quinoxalin-6-amine (**40**) as

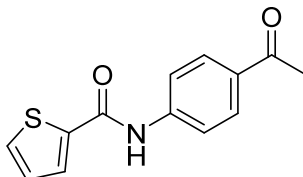
a brown-orange solid (996 mg, 46%). $^1\text{H-NMR}$ (300 MHz, d_6 -DMSO) δ 7.78-7.85 (m, 2H), 7.75 (d, $J=9.0$ Hz, 1H), 7.26 (dd, $J=2.4, 9.0$ Hz, 1H), 6.91 (d, $J=2.3$ Hz, 1H), 6.64 (ddd, $J=1.2, 1.8, 3.4$ Hz, 2H), 6.53 (dd, $J=0.8, 3.4$ Hz, 1H), 6.50 (dd, $J=0.7, 3.4$ Hz, 1H), 6.29 (s, 2H); LC-MS $[\text{MH}]^+$ expected = 278.1 ($\text{C}_{16}\text{H}_{12}\text{N}_3\text{O}_2$), observed = 278.1; HPLC: 88% pure.

***N*-(2,3-Di(furan-2-yl)quinoxalin-6-yl)pyrrolidine-1-carboxamide (23).**¹²⁻¹⁴



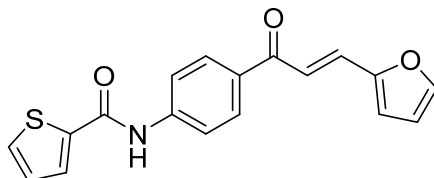
Triethylamine (0.11 mL, 0.79 mmol) was added to a stirring mixture of compound **40** (72.2 mg, 0.261 mmol) and triphosgene (29.1 mg, 0.0981 mmol) in anhydrous DCM (5 mL), and the reaction was stirred for at R.T. (under Ar). After 2 h, pyrrolidine (65.0 μL , 0.79 mmol) was added and the reaction stirred for an additional 4 h. Flash chromatographic purification over silica (hexanes:EtOAc gradient), followed by prep-HPLC purification afforded *N*-(2,3-di(furan-2-yl)quinoxalin-6-yl)pyrrolidine-1-carboxamide (**23**) as an orange solid (34.2 mg, 93%). $^1\text{H-NMR}$ (300 MHz, d_6 -DMSO) δ 8.72 (s, 1H), 8.36 (d, $J=2.0$ Hz, 1H), 8.02 (dd, $J=2.3, 9.2$ Hz, 1H), 7.95 (d, $J=9.0$ Hz, 1H), 7.85-7.89 (m, 2H), 6.62-6.72 (m, 4H), 3.42-3.50 (m, 4H), 1.86-1.93 (m, 4H); LC-MS $[\text{MH}]^+$ expected = 375.2 ($\text{C}_{21}\text{H}_{19}\text{N}_4\text{O}_3$), observed = 375.1; HPLC: 98% pure.

***N*-(4-Acetylphenyl)thiophene-2-carboxamide (41).**



Pyridine (0.39 mL, 4.8 mmol) was added to a stirring mixture of 2-thiophenecarbonyl chloride (0.43 mL, 4.0 mmol) and 2-aminoacetophenone (537 mg, 3.97 mmol) in anhydrous DCM (8 mL) and the reaction was left to stir at R.T. (under Ar). After 4 h, the reaction was extracted into EtOAc and the organics were washed with water and brine, dried over Na_2SO_4 , filtered, and concentrated. Flash chromatographic purification over silica (hexanes:EtOAc gradient) afforded *N*-(4-acetylphenyl)thiophene-2-carboxamide (**41**) as a pale yellow solid (784 mg, 81%). $^1\text{H-NMR}$ (300 MHz, d_6 -DMSO) δ 10.54 (s, 1H), 8.08 (dd, $J=1.1, 3.7$ Hz, 1H), 7.95-8.01 (m, 2H), 7.86-7.93 (m, 3H), 7.25 (dd, $J=3.8, 5.0$ Hz, 1H), 2.55 (s, 3H); LC-MS $[\text{MH}]^+$ expected = 246.1 ($\text{C}_{13}\text{H}_{12}\text{NO}_2\text{S}$), observed = 246.0; HPLC: 99% pure.

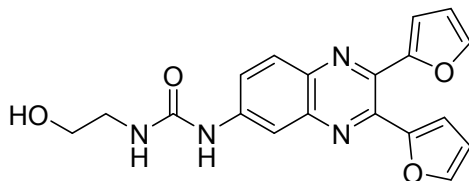
***E*)-*N*-(4-(3-(Furan-2-yl)acryloyl)phenyl)thiophene-2-carboxamide (24).**^{15, 16}



Compound **41** (0.145 mg, 0.591 mmol) and 2-furaldehyde (54.0 μL , 0.652 mmol) were refluxed in a mixture of EtOH (8 mL) in 1 M NaOH (12 mL). After 4 h, the reaction was cooled on ice and the precipitate filtered, rinsed with ice cold EtOH, collected, and dried. Flash chromatographic purification

over silica (hexanes:EtOAc gradient) afforded (*E*)-*N*-(4-(3-(furan-2-yl)acryloyl)phenyl)thiophene-2-carboxamide (**24**) as a yellow solid (140 mg, 73%). ¹H-NMR (500 MHz, *d*₆-DMSO) δ 10.54 (s, 1H), 8.07-8.14 (m, 3H), 7.90-7.97 (m, 4H), 7.53-7.62 (m, 2H), 7.26 (dd, *J*=3.8, 5.0 Hz, 1H), 7.10 (d, *J*=3.5 Hz, 1H), 6.70 (dd, *J*=1.7, 3.5 Hz, 1H), 3.86 (s, 3H); LC-MS [MH]⁺ expected = 324.1 (C₁₈H₁₄NO₃S), observed = 324.0; HPLC: 96% pure.

1-(2,3-Di(furan-2-yl)quinoxalin-6-yl)-3-(2-hydroxyethyl)urea (25**).**¹²⁻¹⁴



Triethylamine (0.29 mL, 2.1 mmol) was added to a stirring mixture of compound **40** (191 mg, 0.691 mmol) and triphosgene (88.8 mg, 0.299 mmol) in anhydrous DCM (7 mL), and the reaction was stirred for at R.T. (under Ar). After 2 h, ethanolamine (0.21 mL, 3.5 mmol) was added and the reaction stirred for an additional 4 h. Flash chromatographic purification over silica (hexanes:EtOAc gradient), followed by prep-HPLC purification, afforded 1-(2,3-di(furan-2-yl)quinoxalin-6-yl)-3-(2-hydroxyethyl)urea (**25**) as a red-orange powder (74.5 mg, 68%). ¹H-NMR (300 MHz, *d*₆-DMSO) δ 9.26 (s, 1H), 8.26 (d, *J*=2.2 Hz, 1H), 7.96 (d, *J*=9.1 Hz, 1H), 7.84-7.89 (m, 2H), 7.72 (dd, *J*=2.3, 9.1 Hz, 1H), 6.67-6.71 (m, 2H), 6.63-6.67 (m, 2H), 6.47 (t, *J*=5.6 Hz, 1H), 4.81 (br s, 1H), 3.45-3.53 (m, 2H), 3.18-3.26 (m, 2H); LC-MS [MH]⁺ expected = 365.1 (C₁₉H₁₇N₄O₄), observed = 365.1; HPLC: 98% pure.

Table S6: Compound characterization data.

#	HPLC Purity	MS Formula	MS Expected	MS Observed
1	99%	C ₂₇ H ₂₅ N ₄ O ₄ S ₂ [MH] ⁺	533.1	533.0
5	99%	C ₁₆ H ₁₀ NO ₄ S ₂ [M-H] ⁻	344.0	343.9
8	99%	C ₂₀ H ₁₀ Br ₂ ClN ₂ O ₂ S ₂ [M-H] ⁻	566.8	566.6
9	99%	C ₂₀ H ₁₅ N ₂ O ₅ [MH] ⁺	363.1	363.0
10	99%	C ₁₉ H ₁₅ N ₂ O ₅ [M-H] ⁻	351.1	351.0
11	99%	C ₁₅ H ₁₀ NO ₅ [M-H] ⁻	284.1	284.0
14	85%	C ₁₈ H ₁₅ N ₄ O ₃ [MH] ⁺	335.1	335.0
15	99%	C ₁₅ H ₁₄ N ₃ O ₂ S [MH] ⁺	300.1	300.0
18	99%	C ₁₆ H ₁₄ N ₃ O ₃ [MH] ⁺	296.1	296.1
19	79%	C ₁₆ H ₁₀ NO ₄ S ₂ [M-H] ⁻	344.0	343.9
20	92%	C ₁₆ H ₁₂ ClN ₂ O ₃ [MH] ⁺	315.1	315.0
23	98%	C ₂₁ H ₁₉ N ₄ O ₃ [MH] ⁺	375.2	375.1
24	96%	C ₁₈ H ₁₃ NO ₃ S [M-H] ⁻	324.1	324.0
25	98%	C ₁₉ H ₁₇ N ₄ O ₄ [MH] ⁺	365.1	365.1
27	94%	C ₂₀ H ₁₉ N ₂ O ₄ S ₂ [MH] ⁺	415.1	415.0
28	78%	C ₇ HBr ₂ O ₃ S ₂ [M-H] ⁻ carbamate fragmented	322.8	322.6
29	99%	C ₂₂ H ₁₄ N ₃ O ₆ [M-H] ⁻	416.1	416.0
31	99%	C ₁₈ H ₁₆ N ₃ O ₃ [MH] ⁺	322.1	322.1
32	99%	C ₂₀ H ₁₇ N ₄ O ₄ [MH] ⁺	377.1	377.0
33	98%	C ₁₇ H ₁₅ BrNO ₄ [MH] ⁺	376.0	375.9
34	84%	C ₂₄ H ₂₂ FN ₄ O ₄ S [MH] ⁺	481.1	481.0
35	97%	C ₁₆ H ₁₄ N ₃ OS ₂ [MH] ⁺	328.1	328.0

References.

1. Johnson, S. M.; Sharif, O.; Mak, P. A.; Wang, H. T.; Engels, I. H.; Brinker, A.; Schultz, P. G.; Horwich, A. L.; Chapman, E. *Bioorganic & medicinal chemistry letters* **2014**, *24*, 786.
2. Parnas, A.; Nadler, M.; Nisemblat, S.; Horovitz, A.; Mandel, H.; Azem, A. *The Journal of biological chemistry* **2009**, *284*, 28198.
3. Galloway, S. M.; Raetz, C. R. *The Journal of biological chemistry* **1990**, *265*, 6394.
4. Vuorio, R.; Vaara, M. *Antimicrob Agents Chemother* **1992**, *36*, 826.
5. Sykes, M. L.; Baell, J. B.; Kaiser, M.; Chatelain, E.; Moawad, S. R.; Ganame, D.; Ioset, J. R.; Avery, V. M. *PLoS Negl Trop Dis* **2012**, *6*, e1896.
6. Sykes, M. L.; Avery, V. M. *Am J Trop Med Hyg* **2009**, *81*, 665.
7. Moffett, R. B. *Organic Syntheses* **2003**, *41*.
8. Koutnikova, H.; Marsol, C.; Sierra, M.; Klotz, E.; Braun-egles, A.; Lehmann, J. WO/2004/072041A1 **2004**.
9. Koutnikova, H.; Sierra, M.; Anne, B.-e.; Marsol, C.; Klotz, E.; Lehmann, J. WO/2004/072046A2 **2004**.
10. Wang, W. L.; Chai, S. C.; Huang, M.; He, H. Z.; Hurley, T. D.; Ye, Q. Z. *Journal of medicinal chemistry* **2008**, *51*, 6110.
11. Hay, M. P.; Turcotte, S.; Flanagan, J. U.; Bonnet, M.; Chan, D. A.; Sutphin, P. D.; Nguyen, P.; Giaccia, A. J.; Denny, W. A. *Journal of medicinal chemistry* **2010**, *53*, 787.
12. Chen, Q. Y.; Bryant, V. C.; Lopez, H.; Kelly, D. L.; Luo, X.; Natarajan, A. *Bioorganic & medicinal chemistry letters* **2011**, *21*, 1929.
13. Rajule, R.; Bryant, V. C.; Lopez, H.; Luo, X.; Natarajan, A. *Bioorgan Med Chem* **2012**, *20*, 2227.
14. Wang, F.; Chen, J.; Liu, X.; Shen, X.; He, X.; Jiang, H.; Bai, D. *Chem Pharm Bull (Tokyo)* **2006**, *54*, 372.
15. Karaman, I.; Gezegen, H.; Gurdere, M. B.; Dingil, A.; Ceylan, M. *Chem Biodivers* **2010**, *7*, 400.
16. Bodiwala, H. S.; Sabde, S.; Gupta, P.; Mukherjee, R.; Kumar, R.; Garg, P.; Bhutani, K. K.; Mitra, D.; Singh, I. P. *Bioorg Med Chem* **2011**, *19*, 1256.